astro8405

An Introduction to the

Cosmic Microwave Background

Kaustuv Basu

kbasu@uni-bonn.de

eCampus | Lernplattform der Universität Bonn

astro8405: The Cosmic Microwave Background

Aktionen

This course intends to give you a modern and up-to-date introduction to the science and experimental techniques relating to the Cosmic Microwave Background. No prior knowledge of cosmology is necessary, your prerequisite are a basic understanding of electrodynamics and thermal physics and some familiarity with Python programming.

Lecture 11:

Part 1: CMB map-making

Part 2: Anomalies and non-Gaussianity

The steps for CMB data analysis

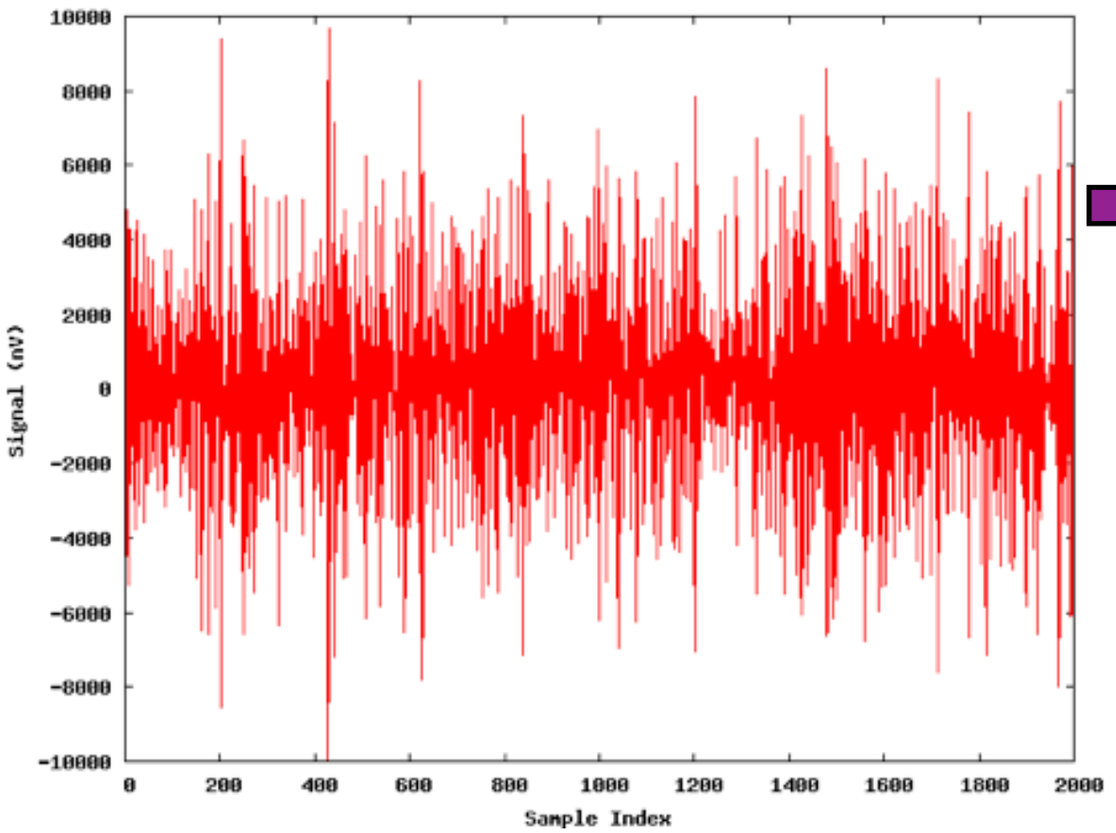

Time-series data or
Time-ordered data (TOD)

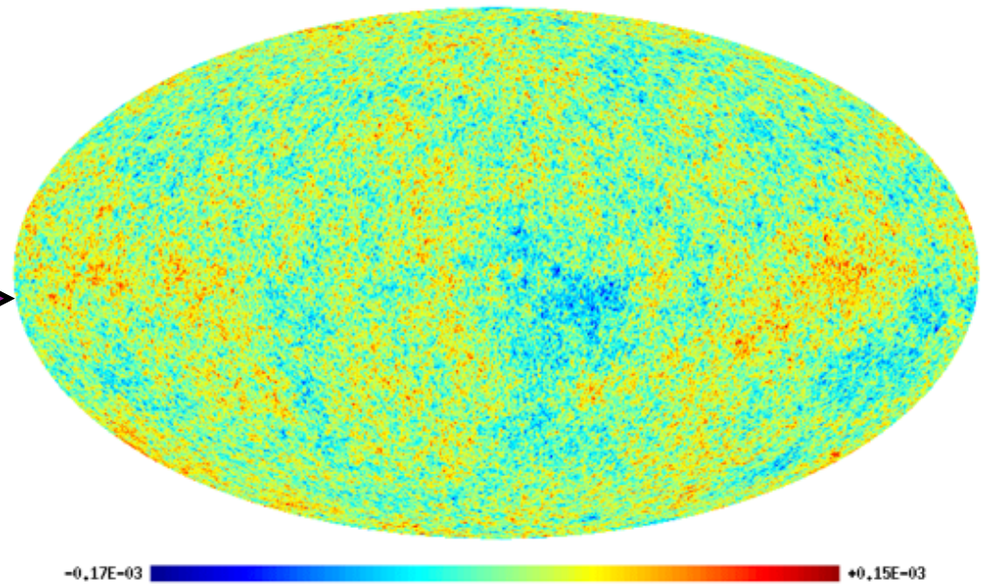

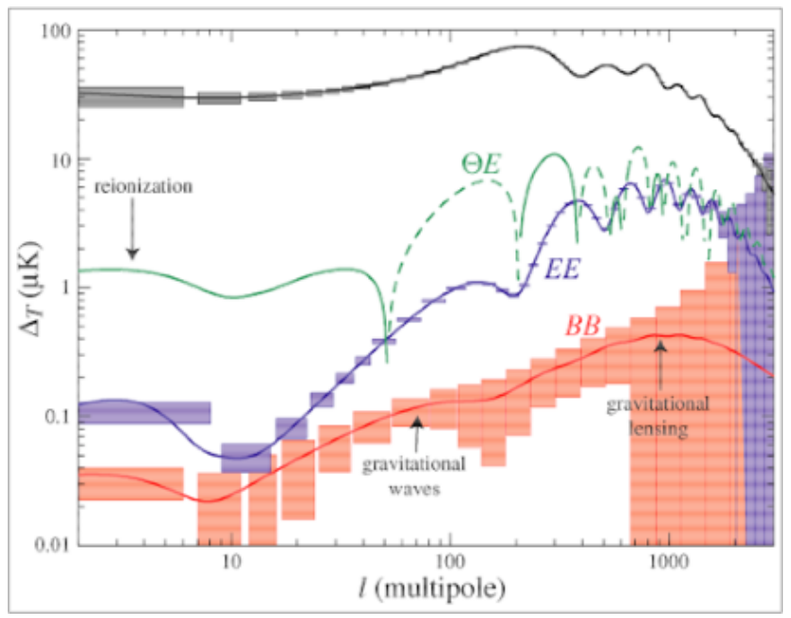

Why we need a map?

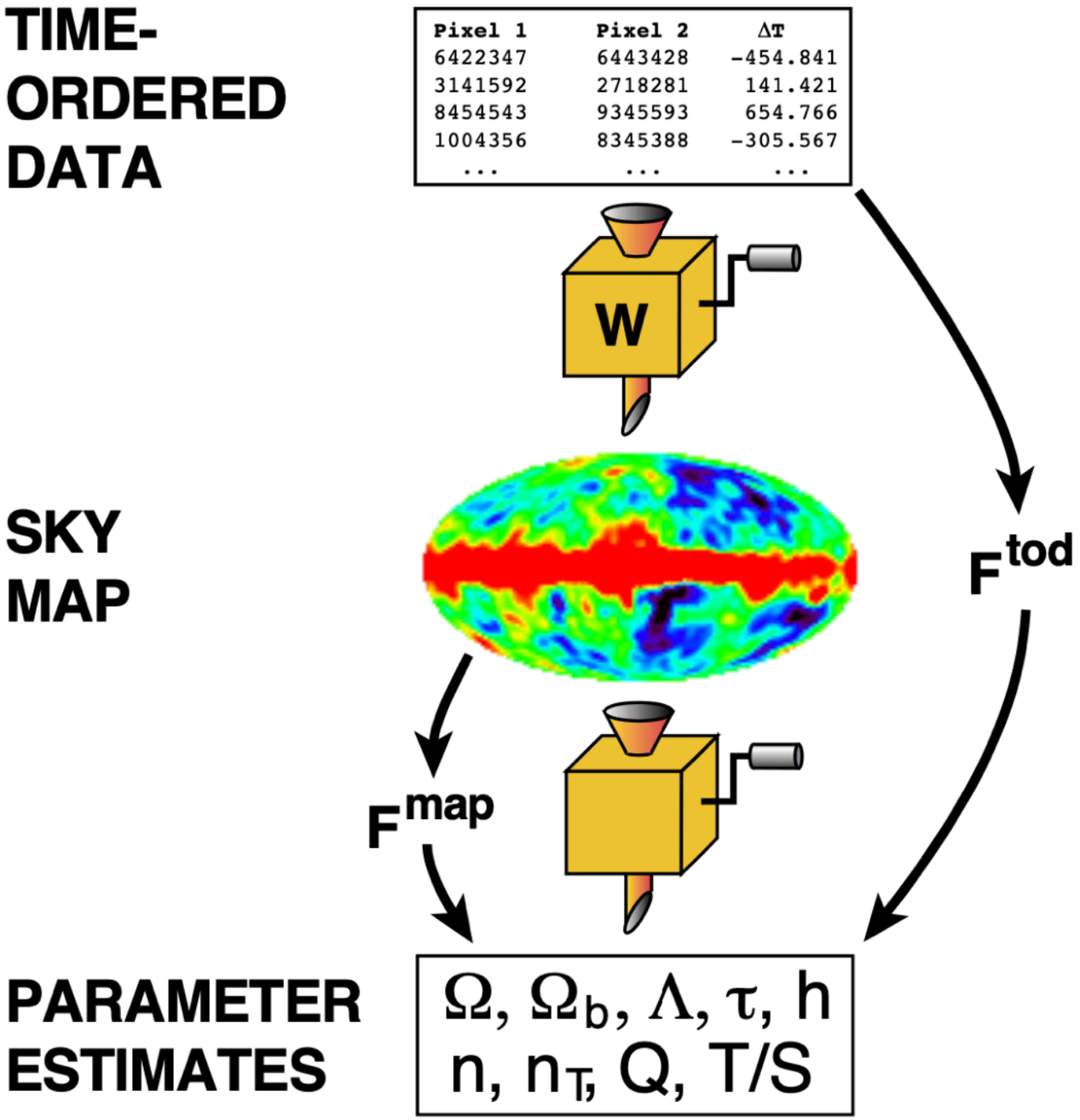

Map-making can be thought as a general problem of linear transform which produces from n numbers $y_1, y_2, \ldots, y_n$ as raw data or time-ordered data, to m numbers $x_1, x_2, \ldots, x_m$ in the map-space or pixel space:

$$\boldsymbol{y} = \mathbf{A}\boldsymbol{x} + \boldsymbol{n}$$

This transformation is always associated with some information loss. However, we generally do not have a complete understanding of all the signal and noise properties to make direct use of the time-series data for cosmological analysis.

From Tegmark (1997)

Removal of (correlated) atmospheric noise

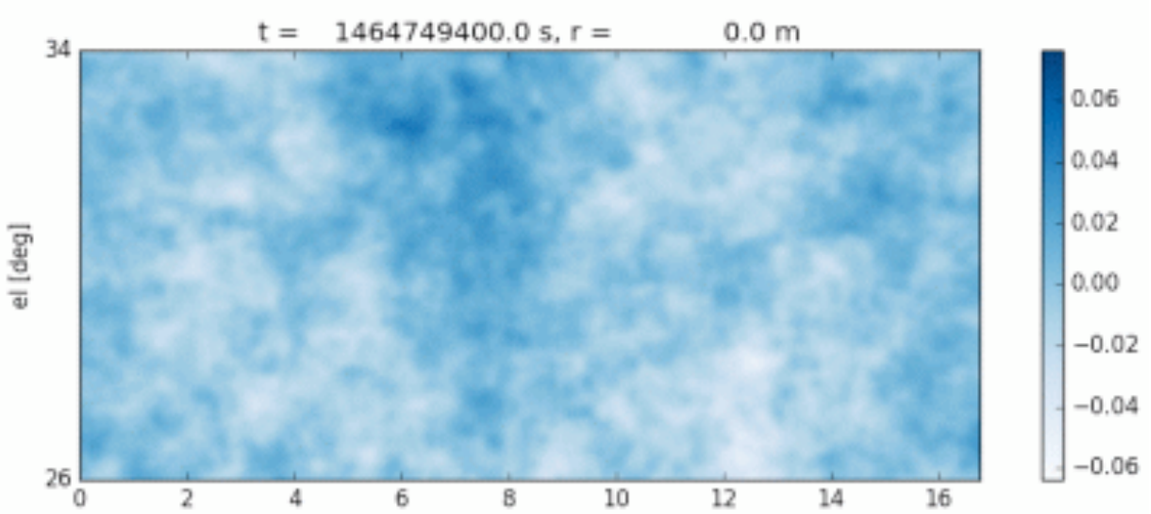

The telescope's view through one realization of turbulent, wind-blown, atmospheric water vapor. The volume of atmosphere being simulated depended on (a) the scan width and duration and (b) the wind speed and direction

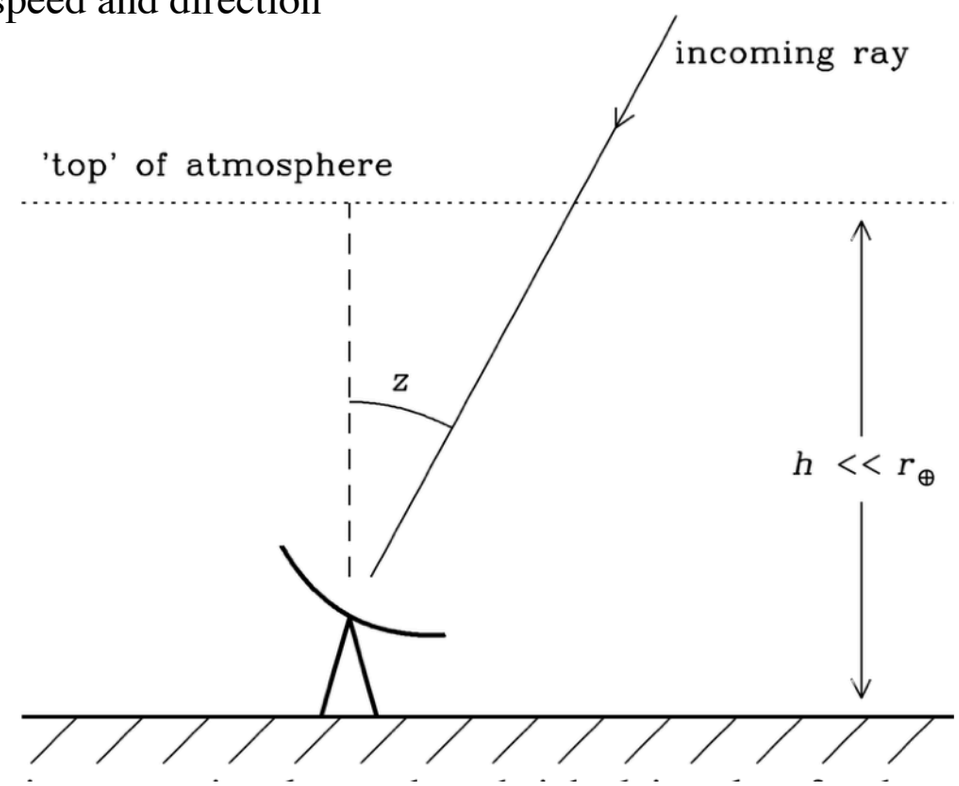

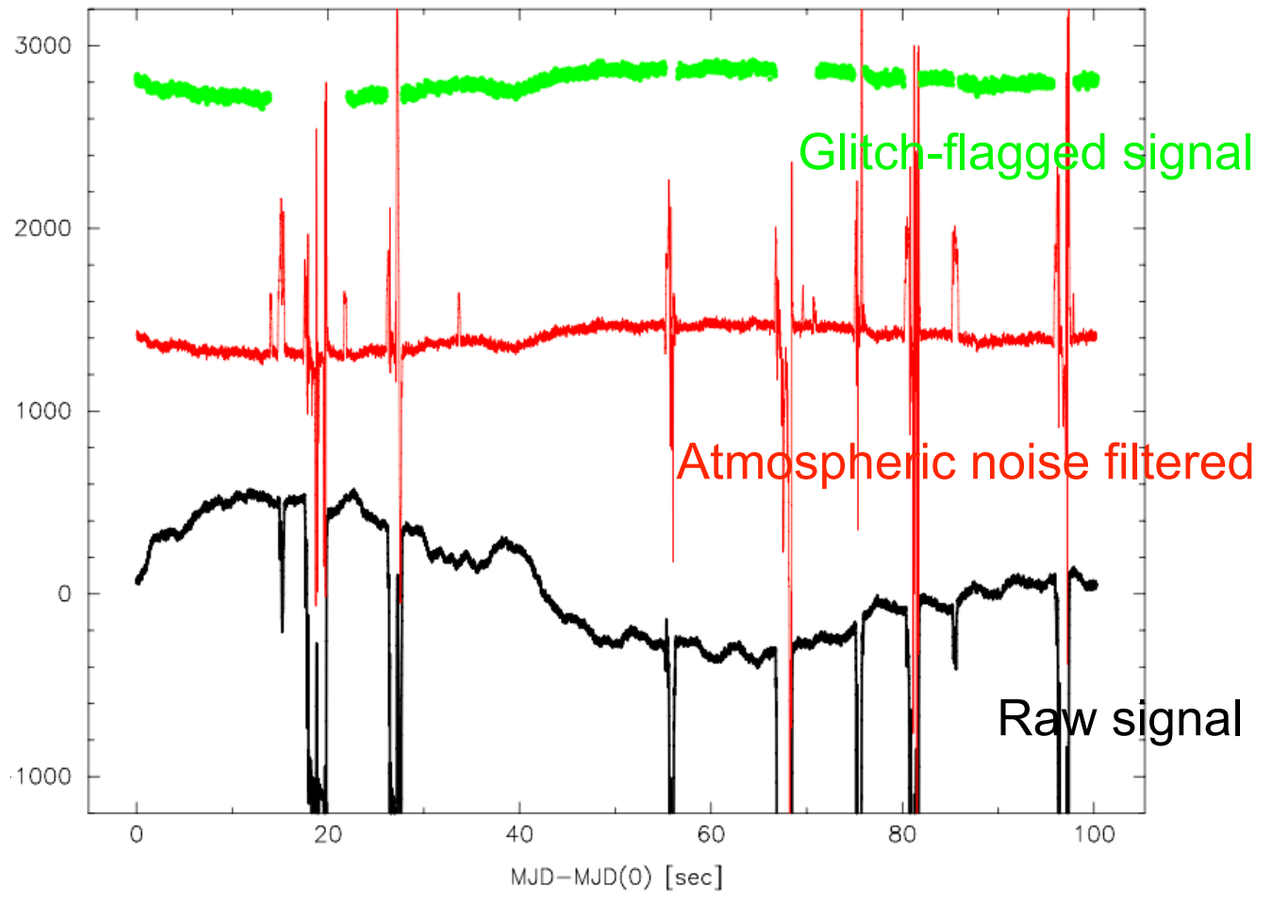

Martin Sommer, PhD thesis

An example of TOD filtering

The time-series data from a subset of bolometers in the APEX-SZ experiment

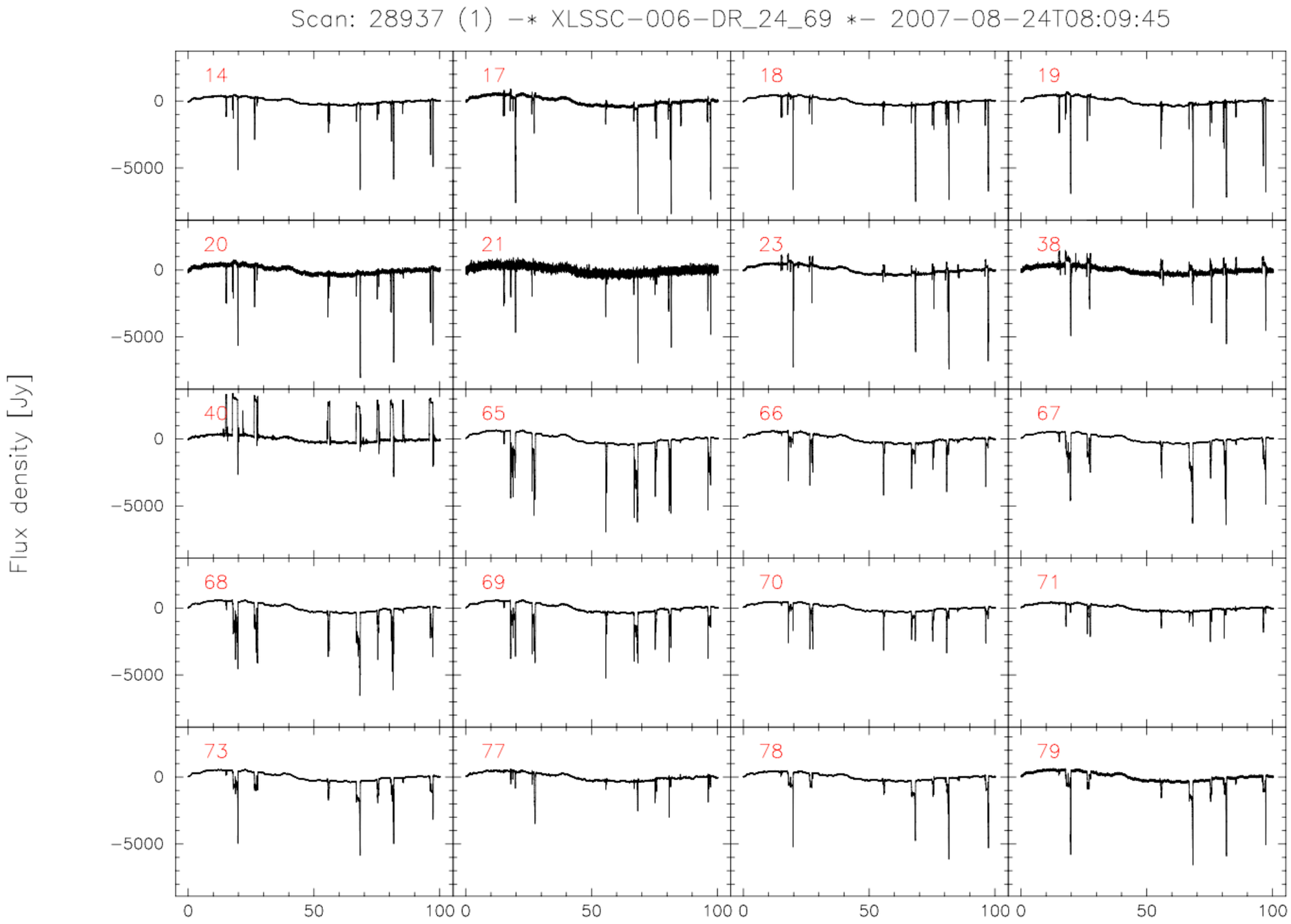

Martin Sommer, PhD thesis

An example of TOD filtering

The same time-series data after the removal of correlated atmospheric noise

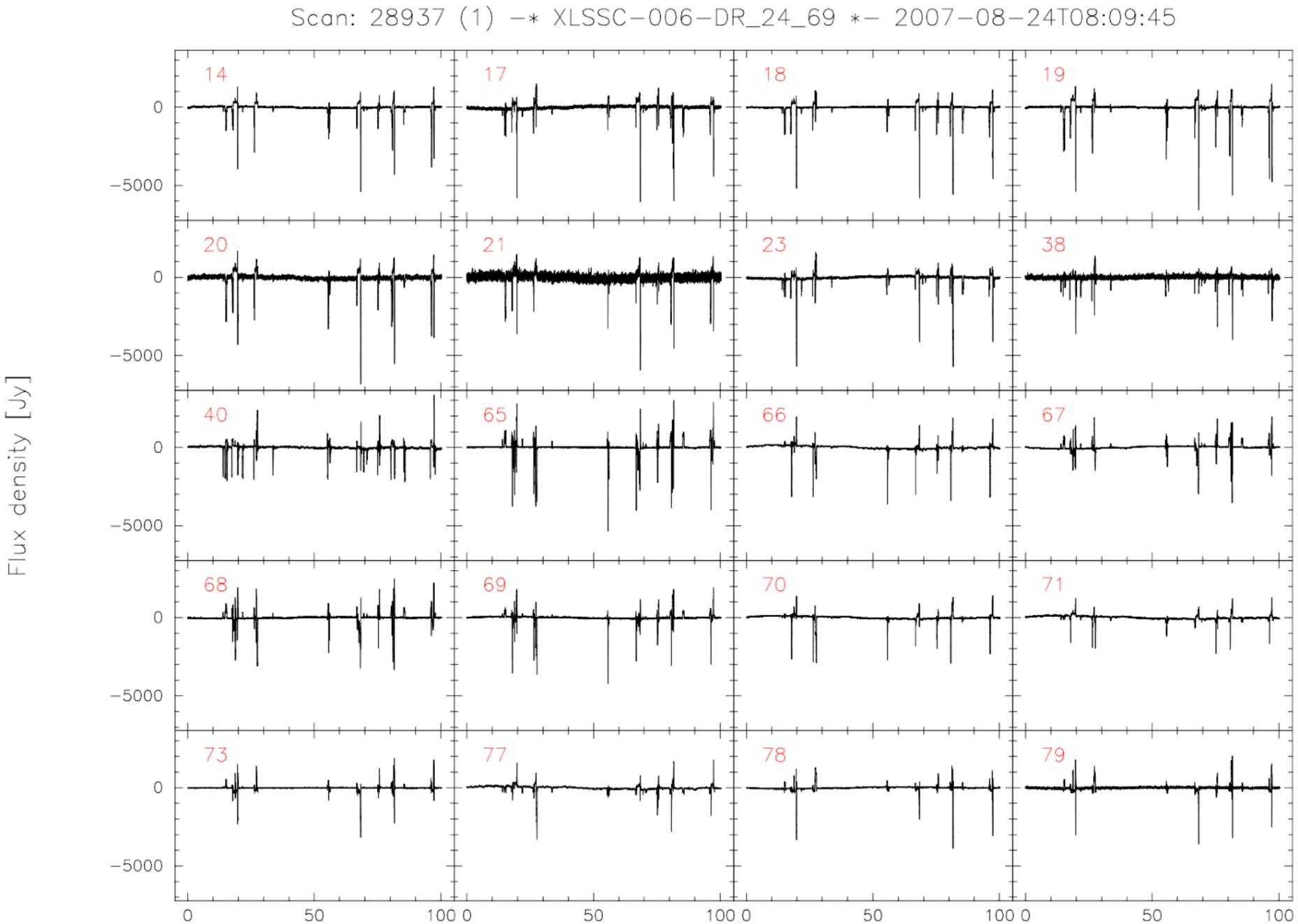

Martin Sommer, PhD thesis

An example of TOD filtering

Now after removal of glitches in the time streams

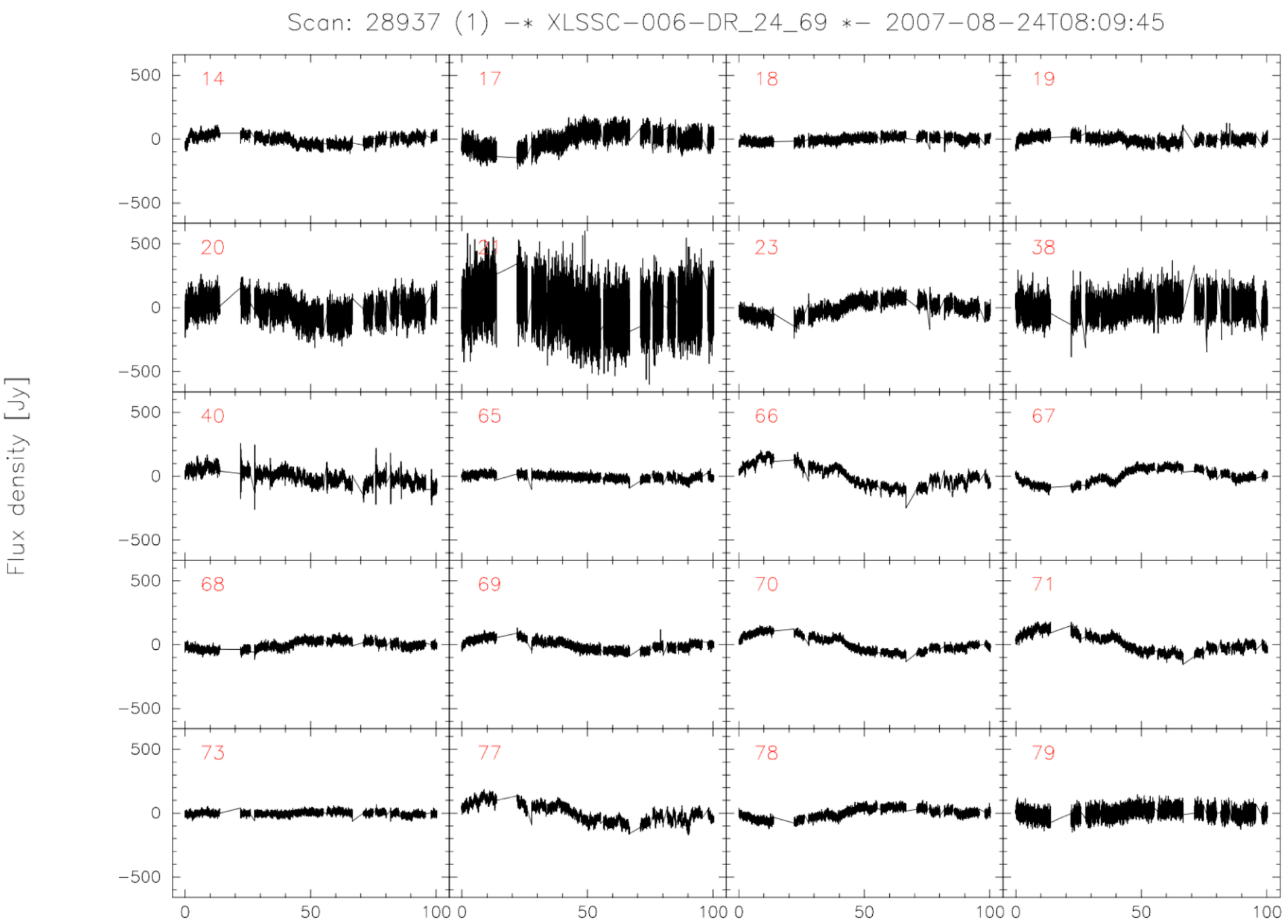

Martin Sommer, PhD thesis

Deglitching

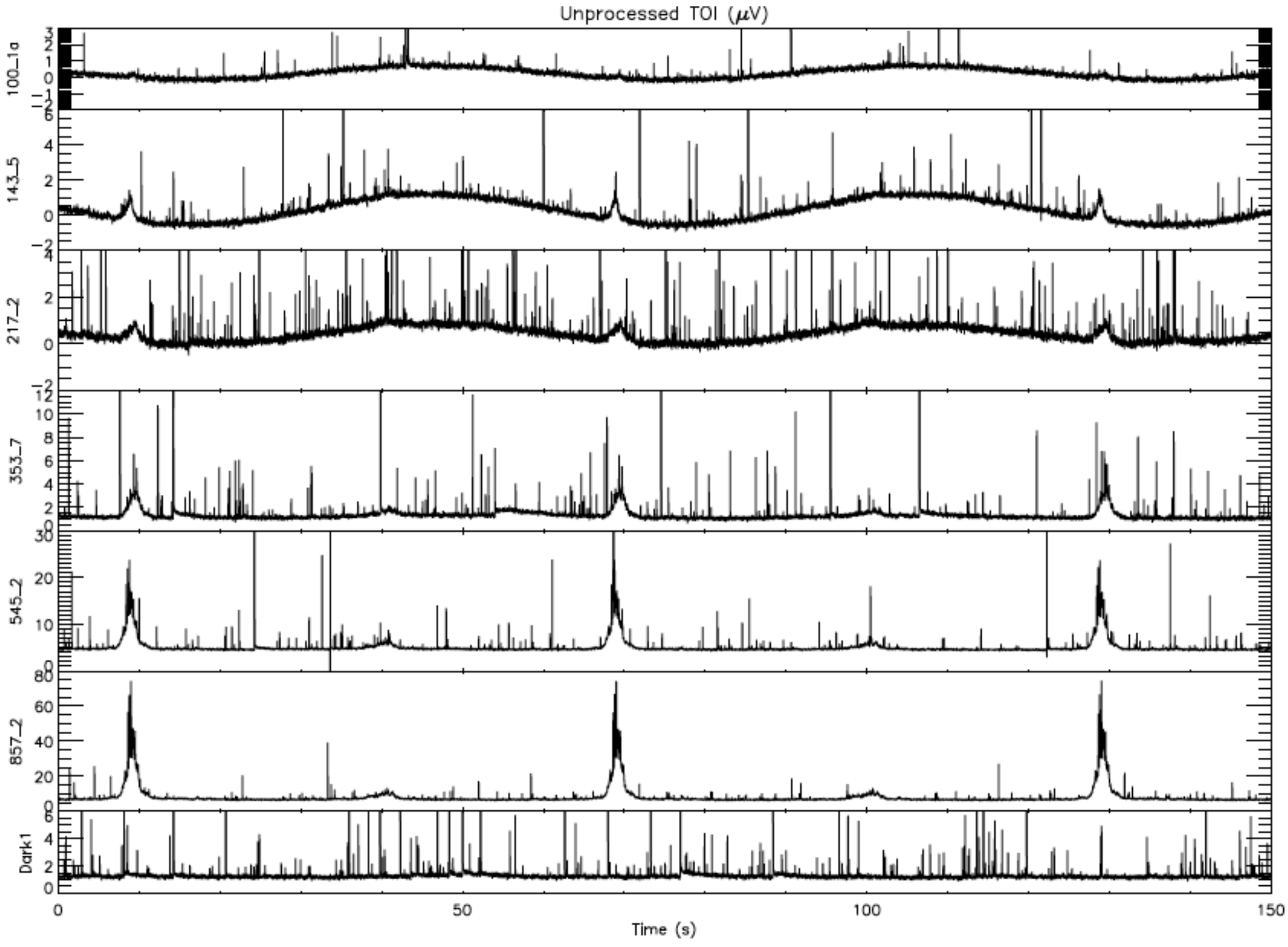

Figure 13. Examples of raw (unprocessed) TOI for one bolometer at each of six HFI frequencies and one dark bolometer. Slightly more than two scan circles are shown. The TOI is dominated by the CMB dipole, the Galactic dust emission, point sources, and glitches. The relative part of glitches is over represented on these plots due to the thickness of the lines that is larger than the real glitch duration.

Planck TOI data & differential noise

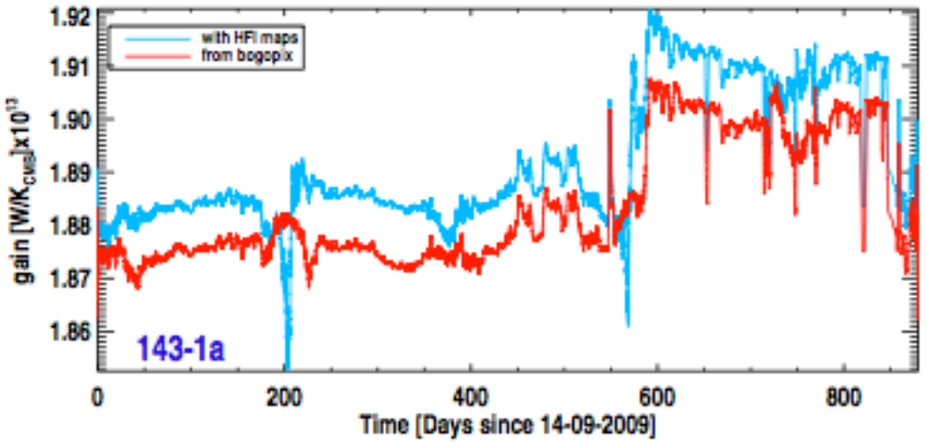

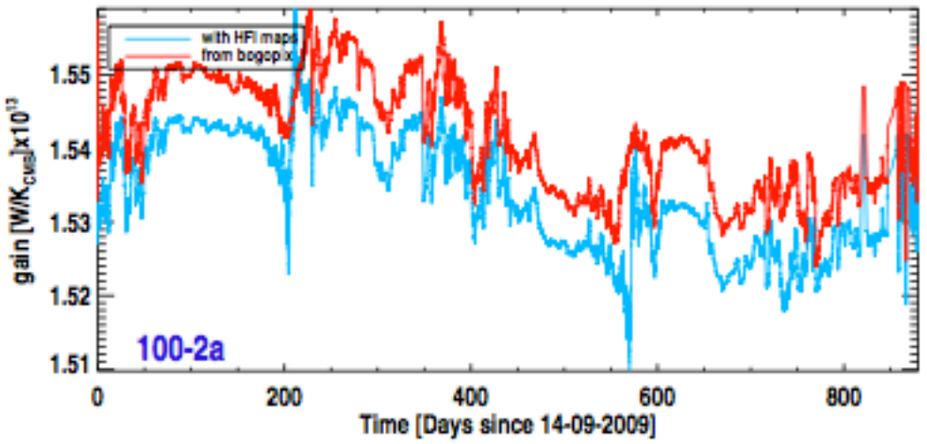

Figure 7. Example of results from `bogopix` obtained for two HFI detectors, compared with those of the Solar dipole calibration. Gain values for individual rings have been smoothed with a width of 50 rings (~ 2 days), to increase the signal-to-noise ratio of the plots. We observe a good agreement between `bogopix` results and those obtained with the HFI maps, for the relative gain variation, except for the time intervals where the Solar dipole's amplitude is low with respect to the Galactic emission. The averaged value of the gains are, however, offset by factors (different from one detector to the other) of the order of 0.5 to 1 %.

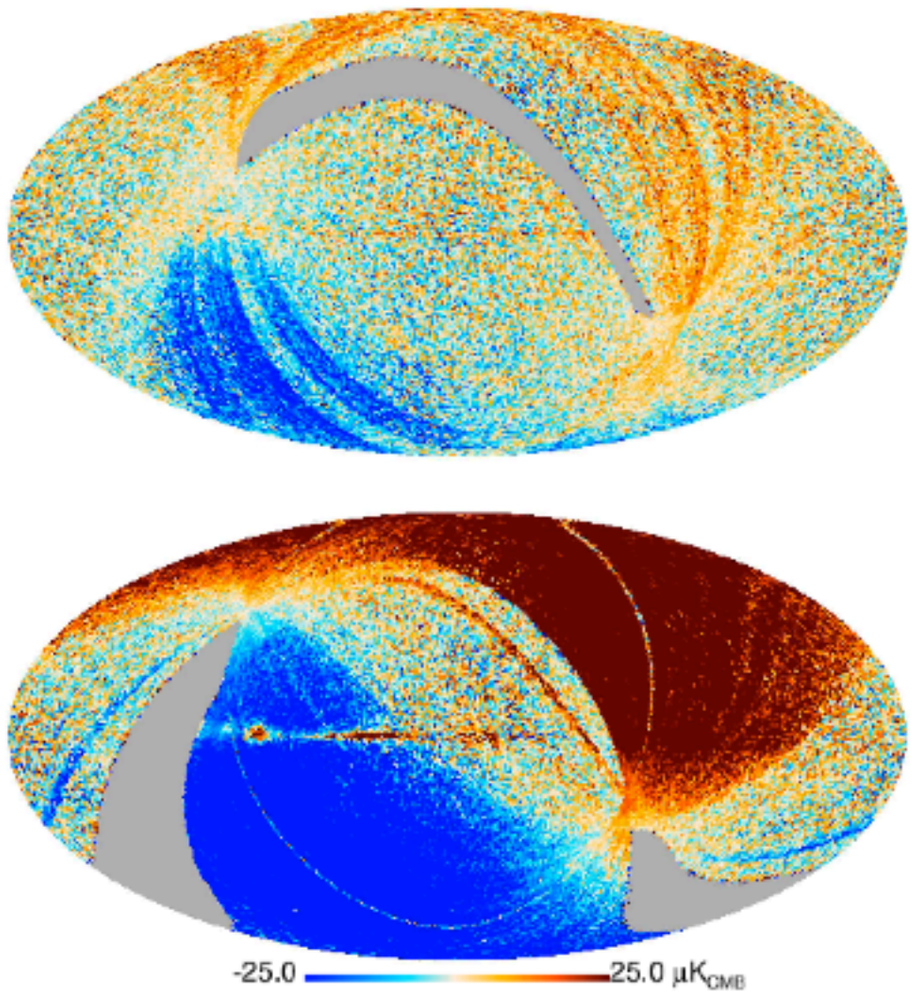

Figure 4. Differences between temperature maps built using data from detector 143-1a, for surveys 1 and 3 (top) and 2 and 4 (bottom). In both cases, large scale features appear. Their amplitude and disposition on the sky are compatible with residuals from the Solar dipole, due to time variations of the detector gain, of the order of 1 to 2 % These residuals should be compared to the amplitude of the Solar dipole, 3.353 mK_{CMB}.

Planck scanning strategy

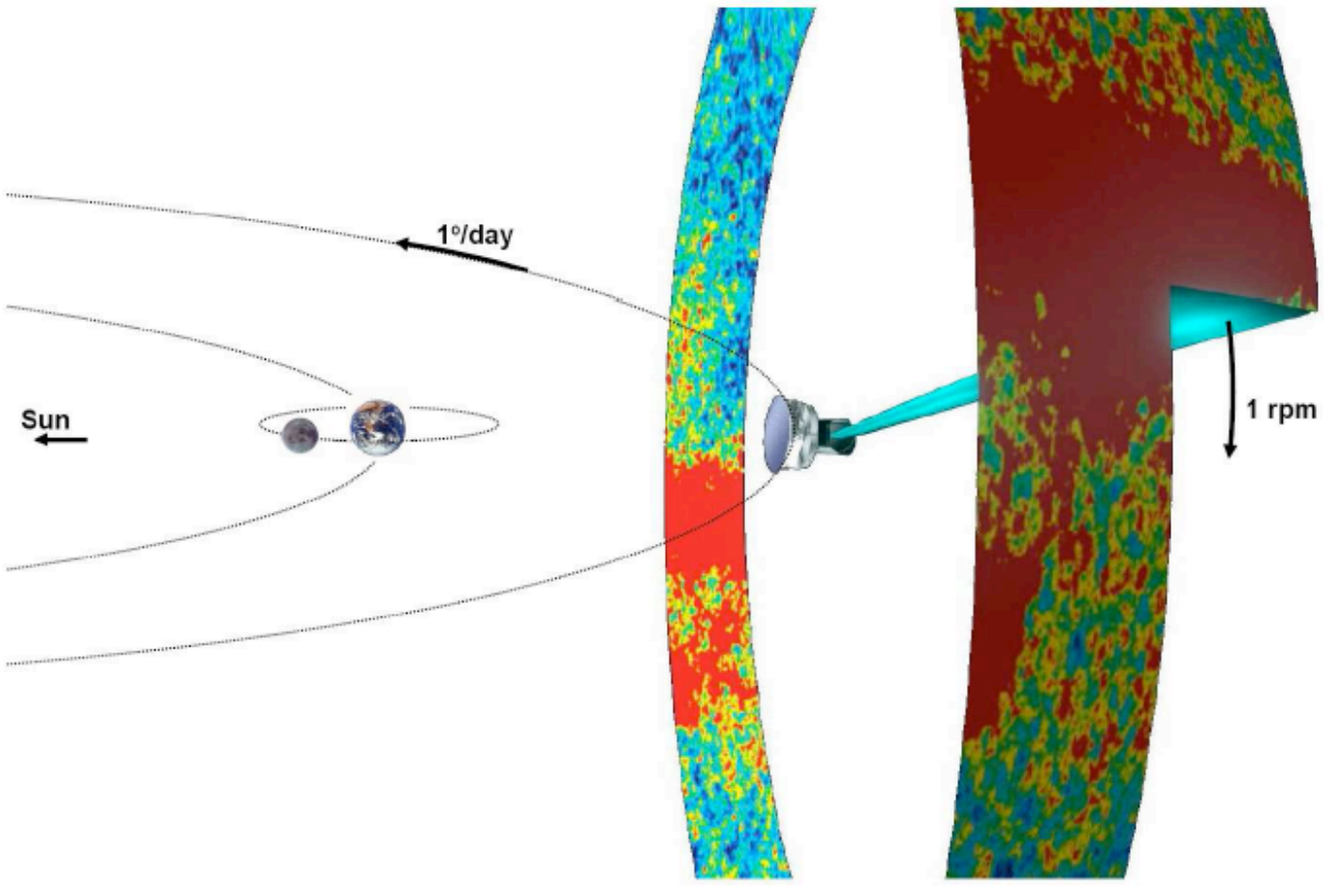

Simplified way to show the Planck scanning strategy, without additional motion of the spin axis

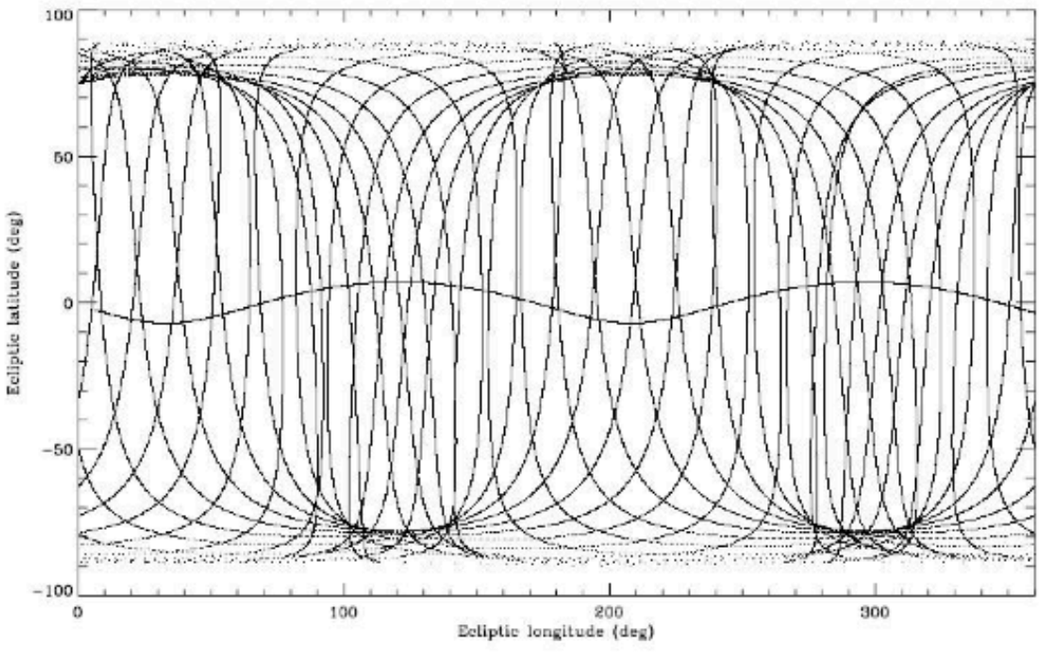

Spin axis path with a 7 degree amplitude cycloidal scanning, from #dupac2005

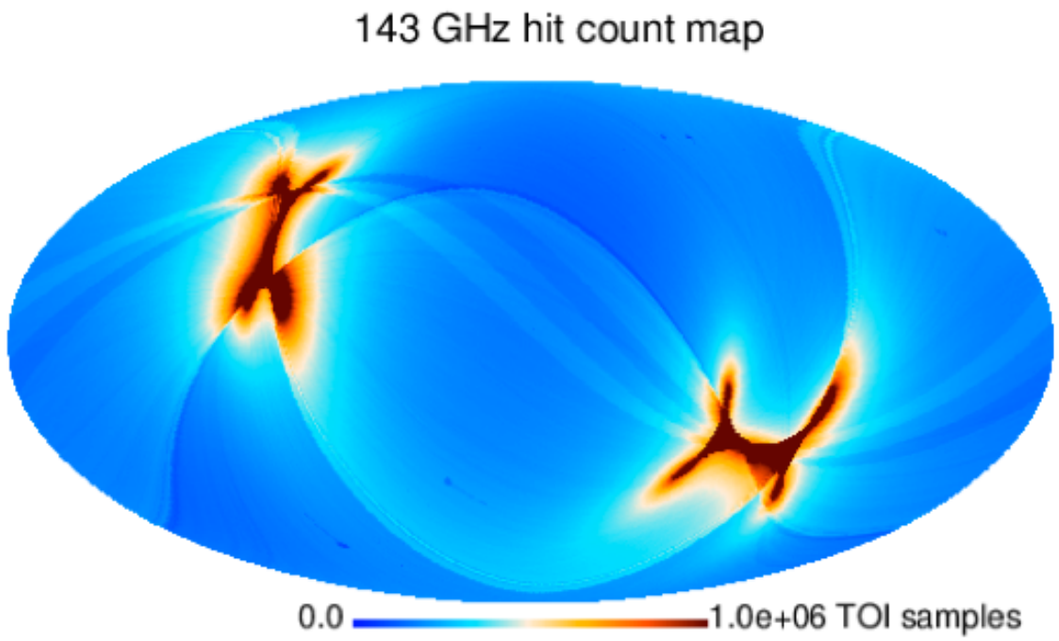

De-striping, or the removal of scanning artefacts

Common to get stripes in the scan direction.

Removal easy in Fourier space.

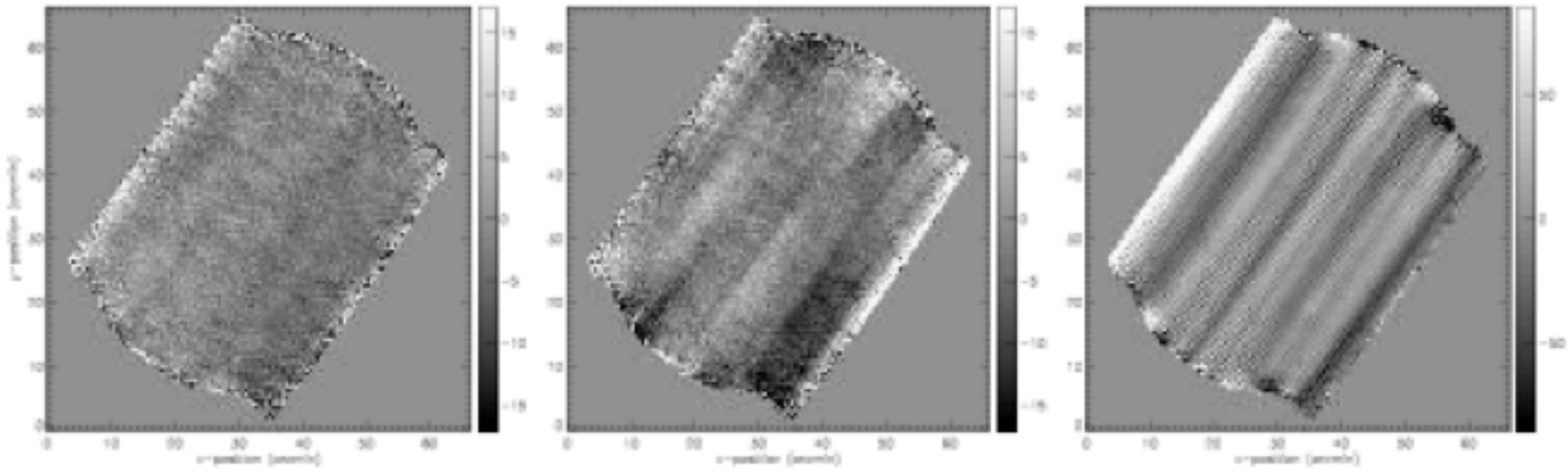

map space

Fourier transformation also helps to separate signal and noise better (different temporal signal).

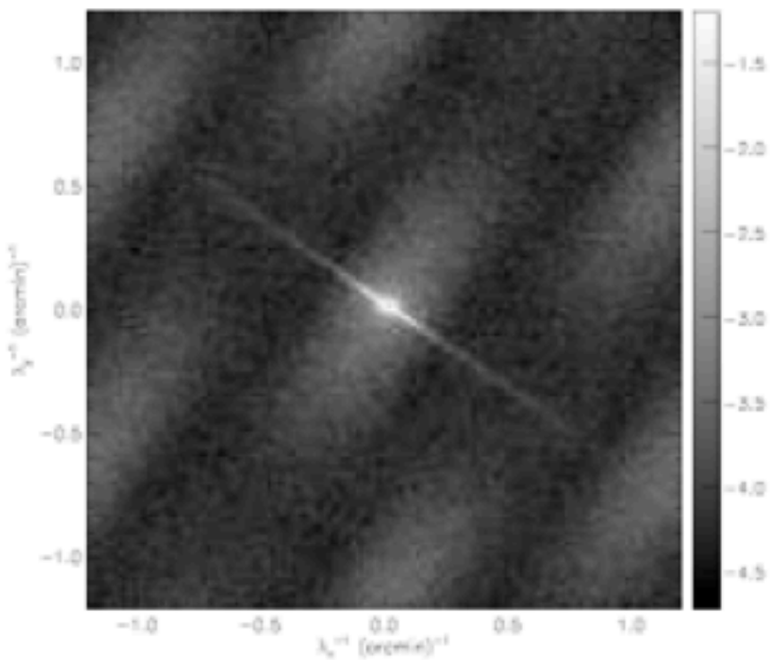

Fourier space

Patanchon et al ; BLAST data

De-striping, or the removal of scanning artefacts

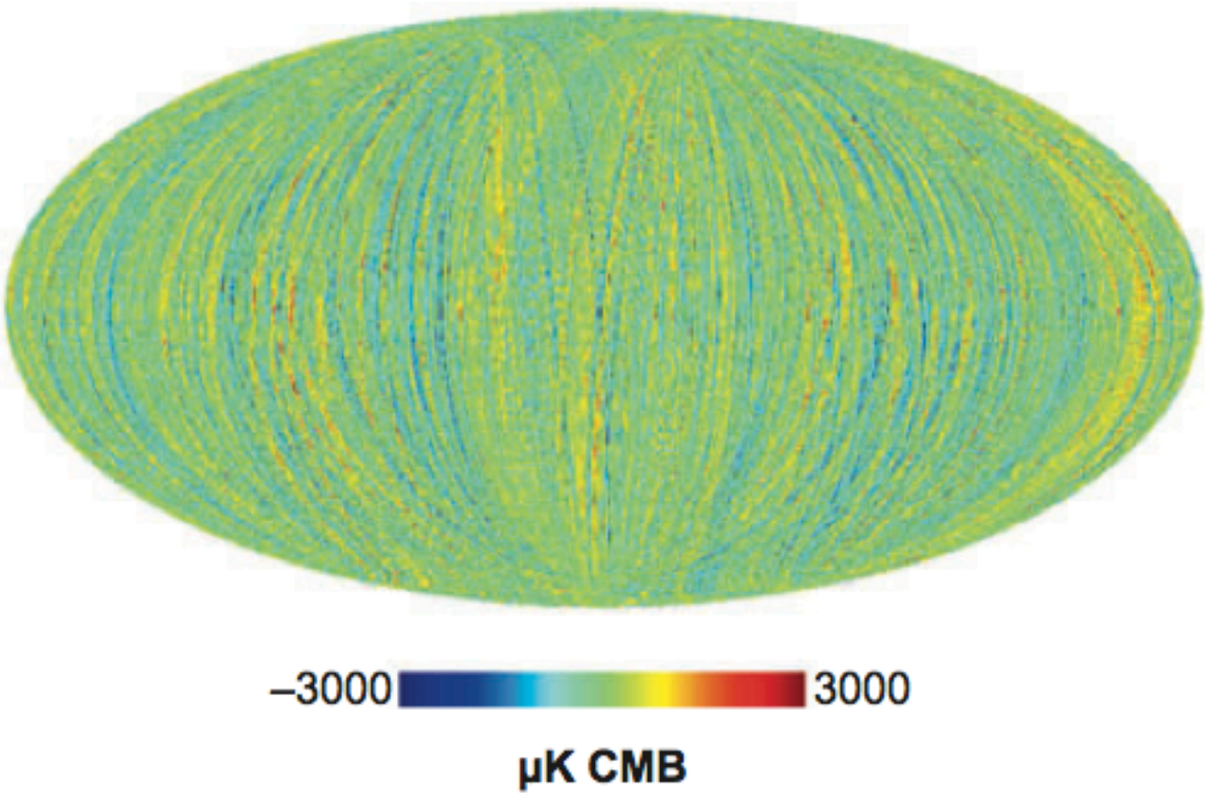

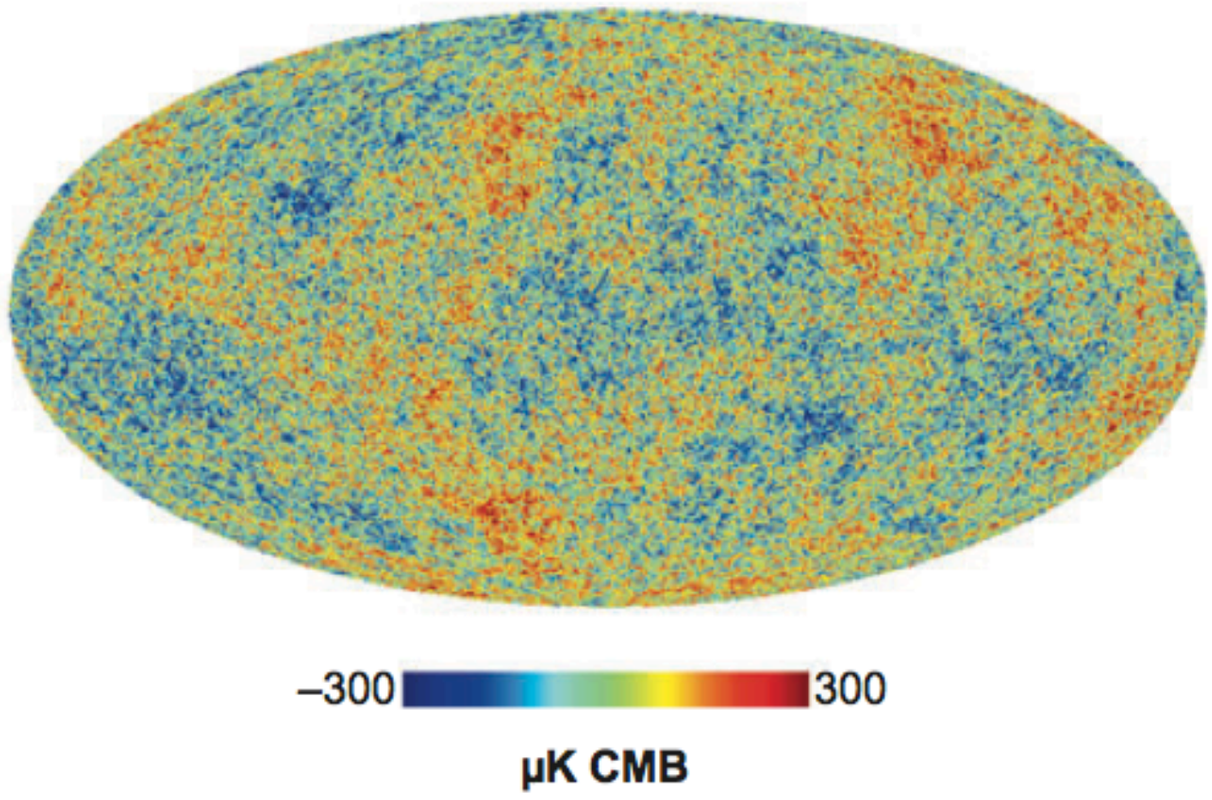

Figure 10

Effect of destriping on simulated sky maps. (*Left*) Map from a raw time stream. (*Right*) Map after applying a destriping algorithm (note the different scales). This simulation was done for the Planck High Frequency Instrument (38).

Figure taken from Samtleben et al. 2007.

Planck sky maps

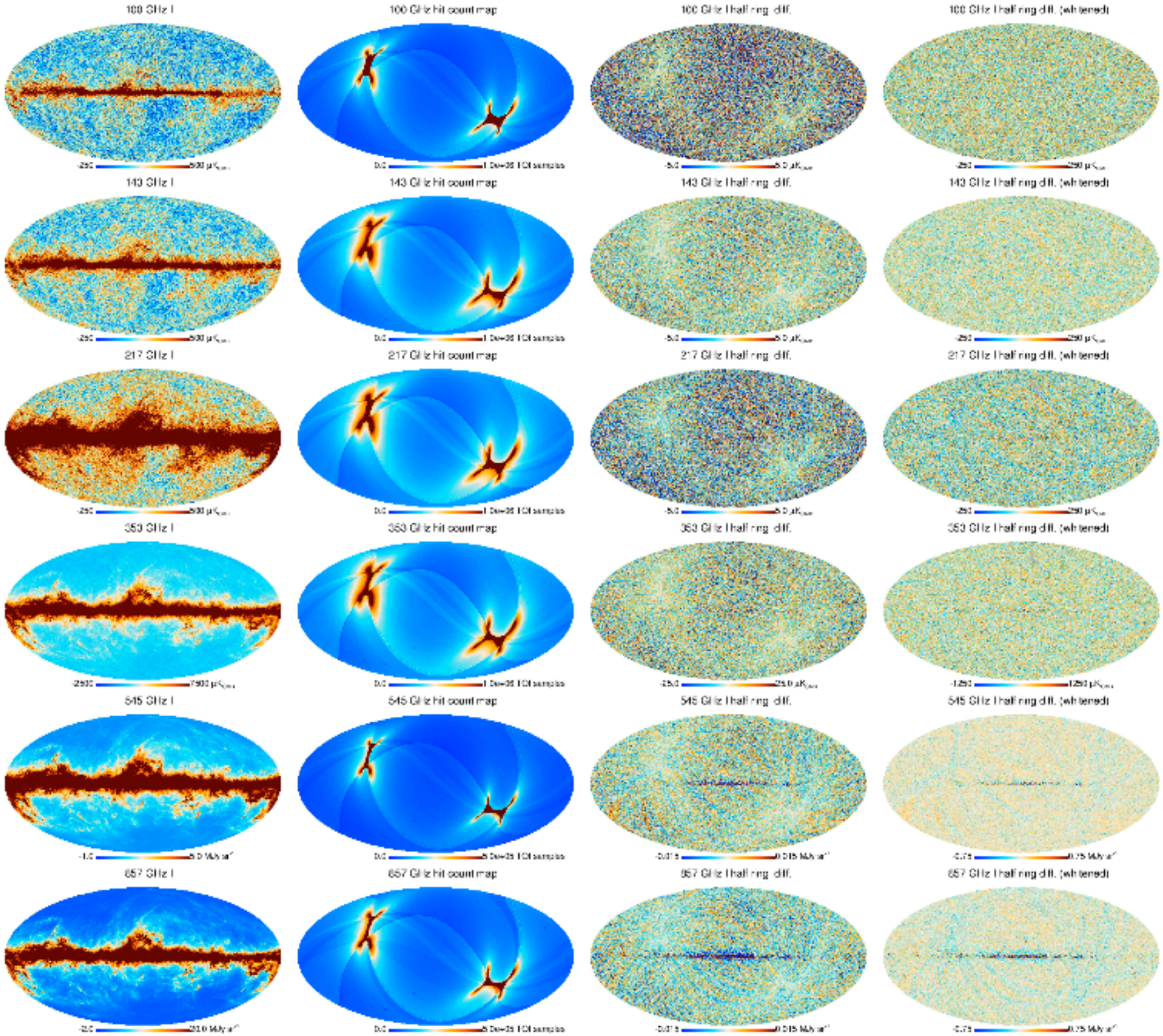

Planck collaboration (2013)

CMB “anomalies” and non-Gaussianity

CMB is Gaussian random field

The CMB data is perfectly described as a Gaussian random field, originating from stochastic density fluctuations created by inflation and enhanced by baryonic interactions.

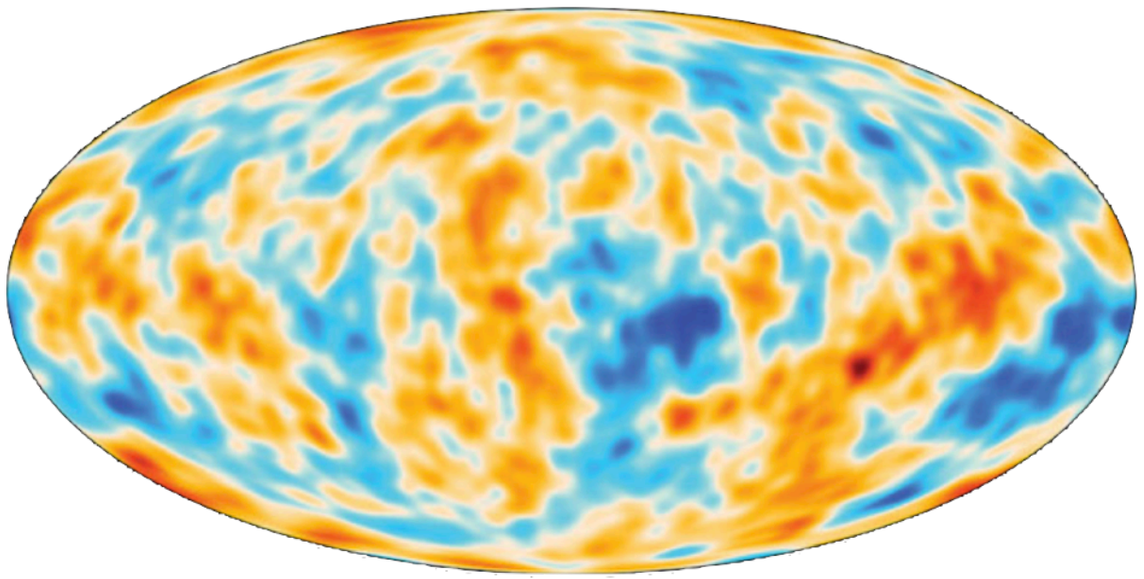

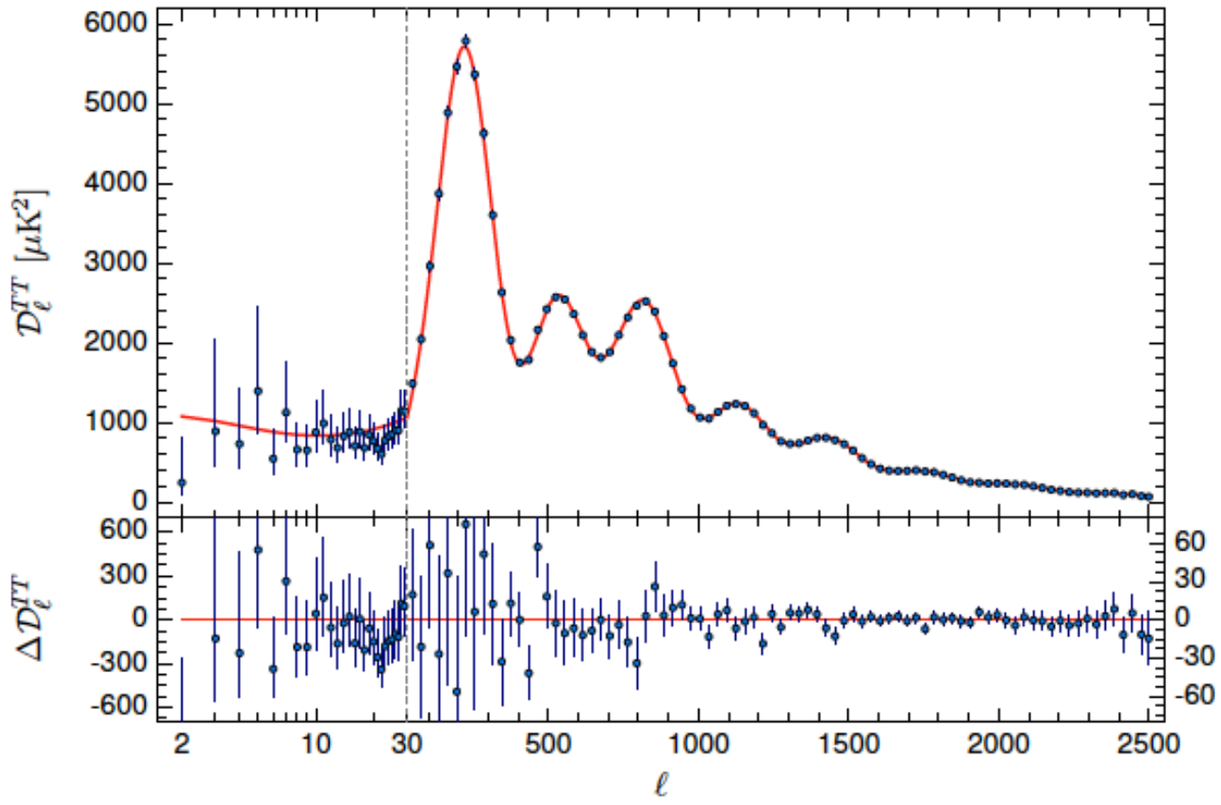

Smoothed CMB map (above), TT (right above), TE (right), and EE (far right) angular power spectrum measurements from *Planck* satellite data, fitted with a 6-parameter ΛCDM cosmology model.

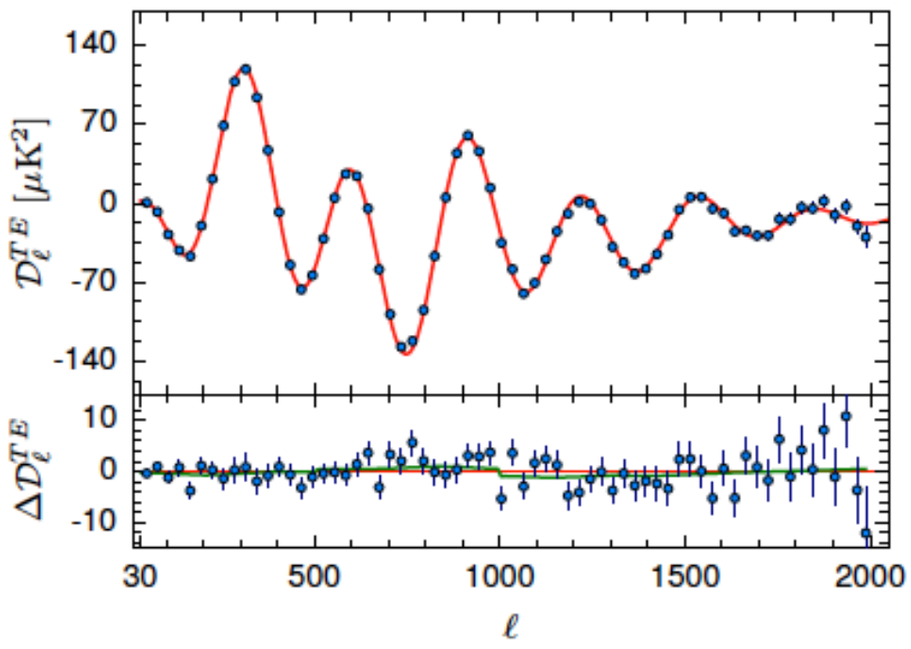

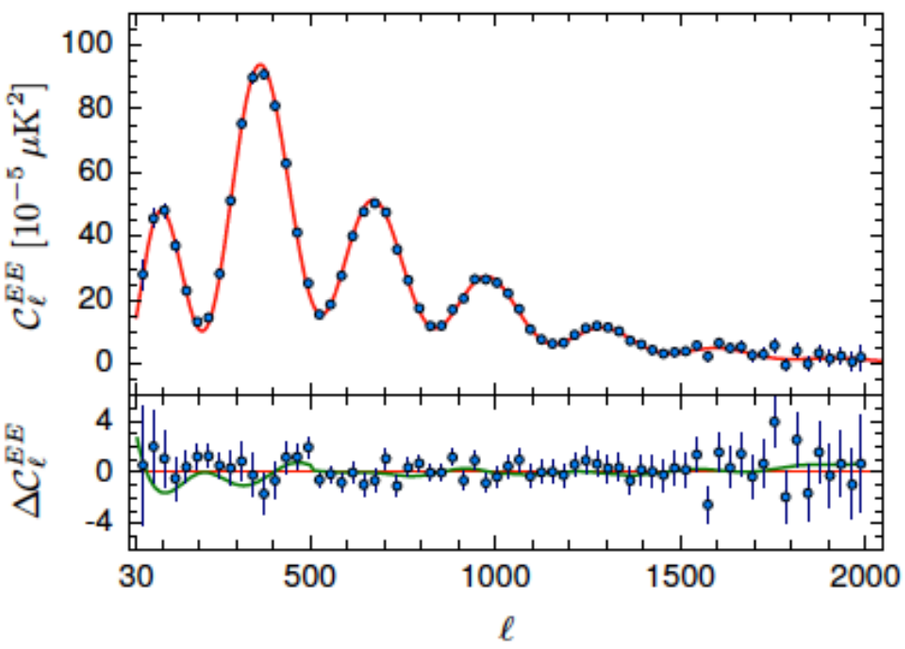

Low multipole “anomaly”

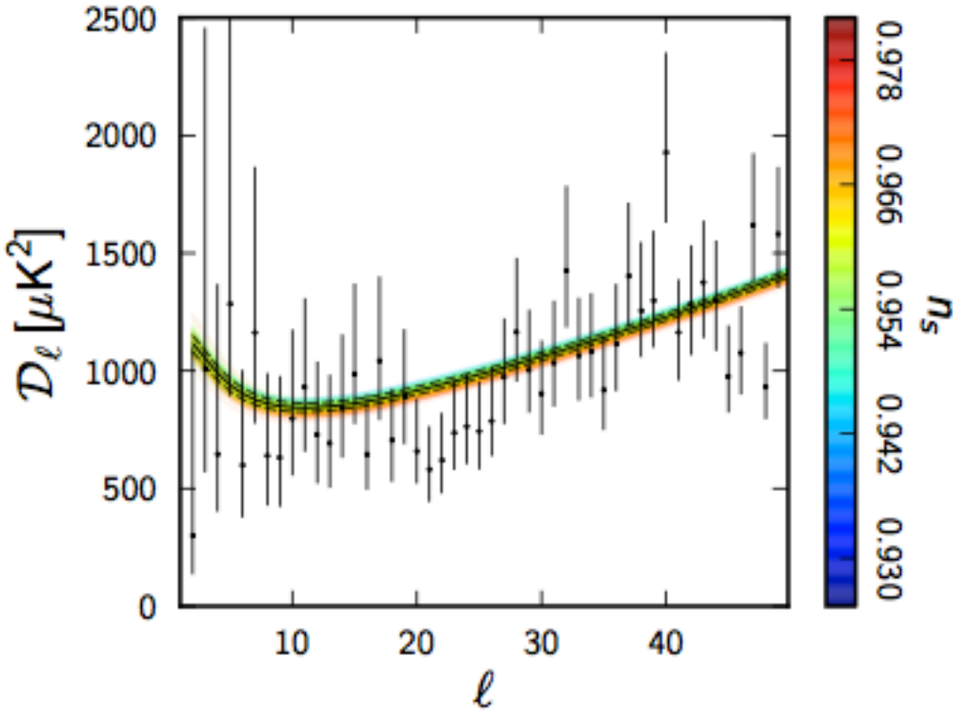

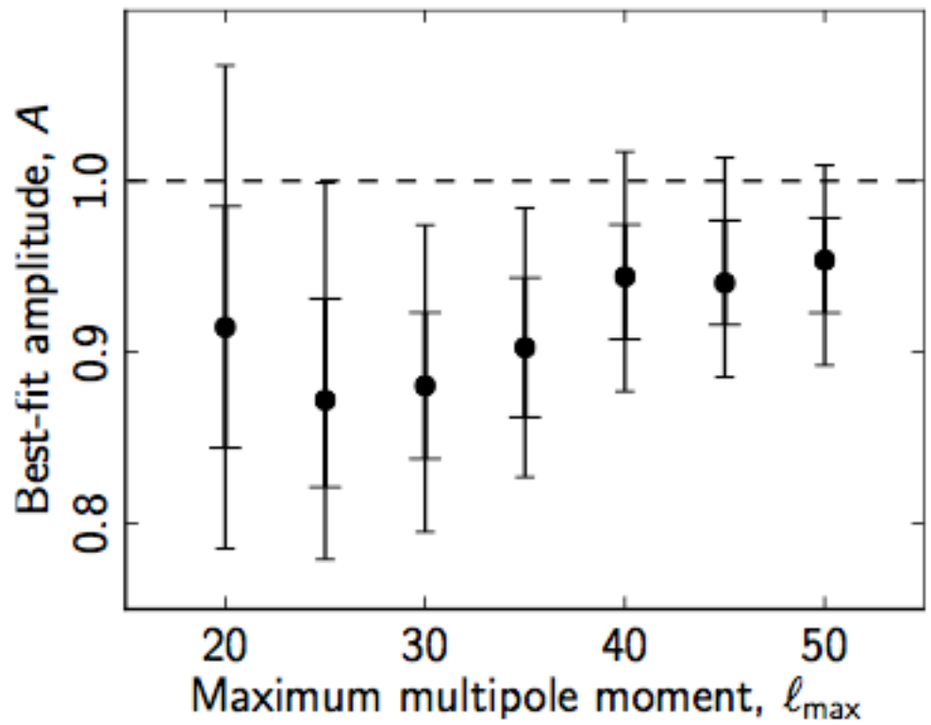

Planck collaboration (2013)

Fig. 39. *Left*: *Planck TT* spectrum at low multipoles with 68% ranges on the posteriors. The “rainbow” band show the best fits to the entire *Planck*+WP likelihood for the base ΛCDM cosmology, colour-coded according to the value of the scalar spectral index n_s. *Right*: Limits (68% and 95%) on the relative amplitude of the base ΛCDM fits to the *Planck*+WP likelihood *fitted only to the Planck TT likelihood* over the multipole range $2 \le \ell \le \ell_{max}$.

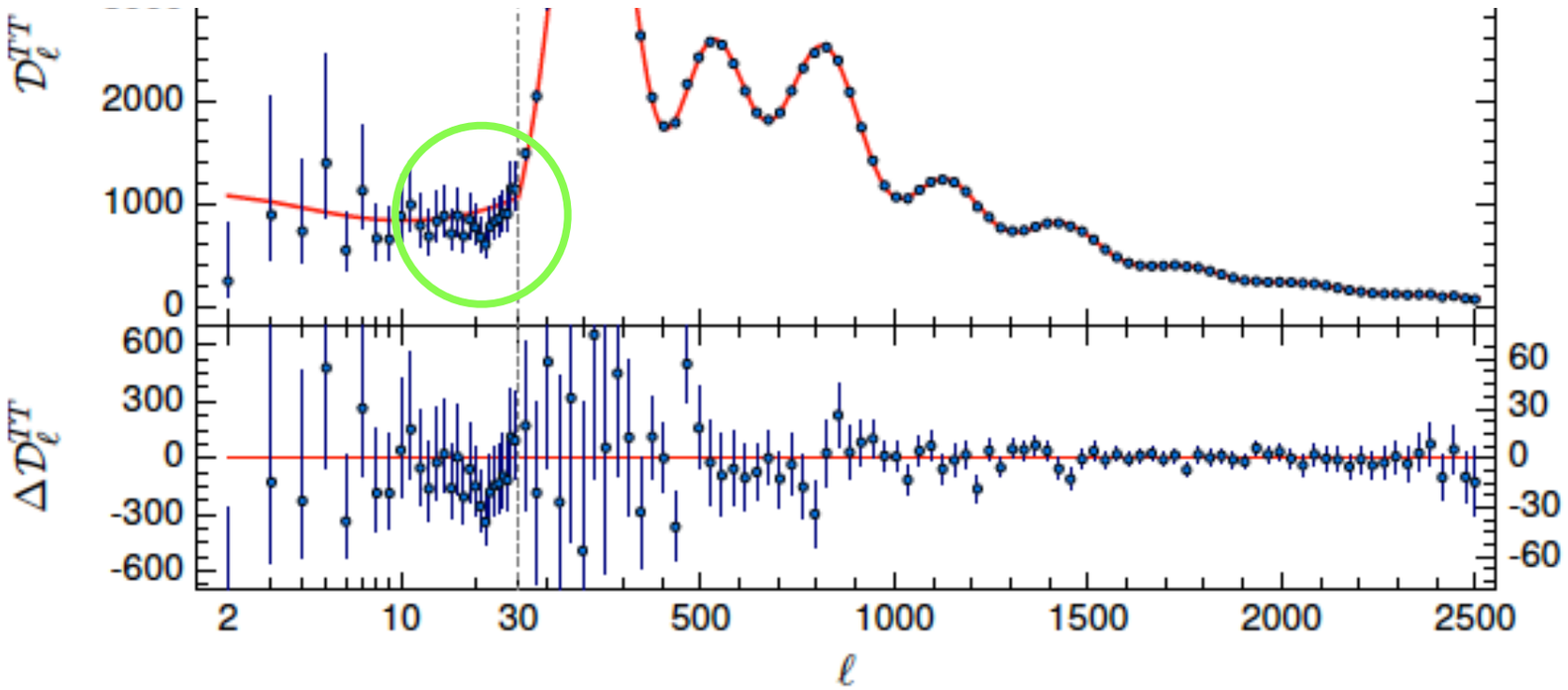

Low multipole “anomaly”

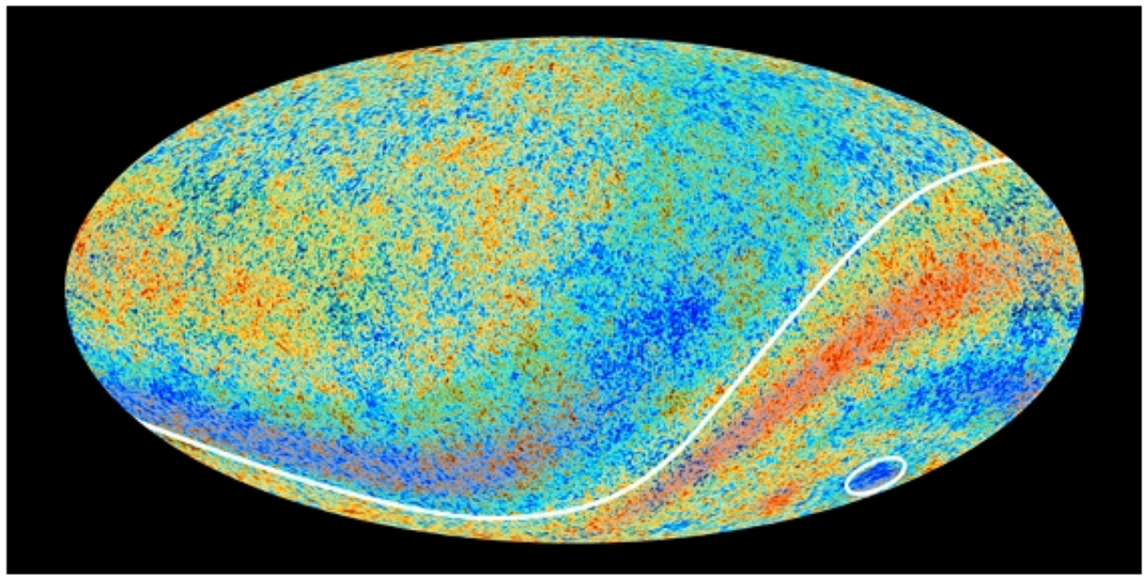

Planck’s anomalous sky: the hemispheric asymmetry and the cold spot. *Credit: ESA and the Planck Collaboration*

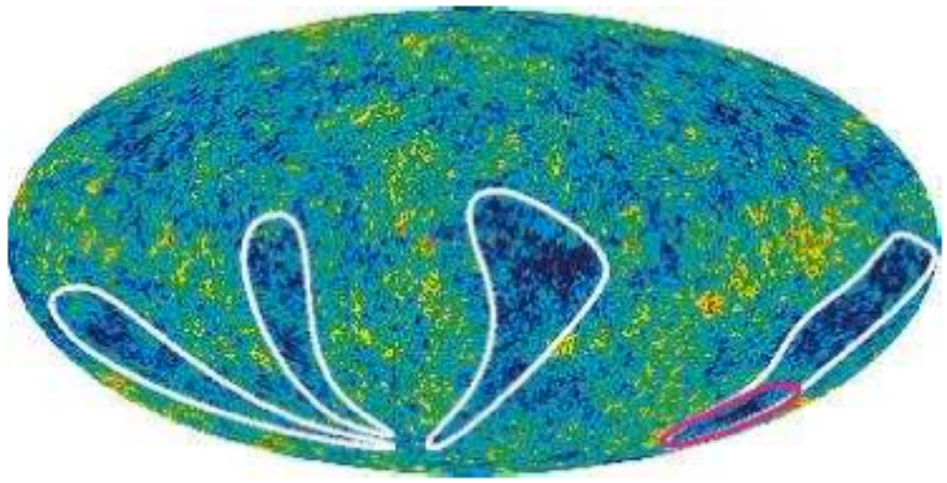

WMAP “fingers”

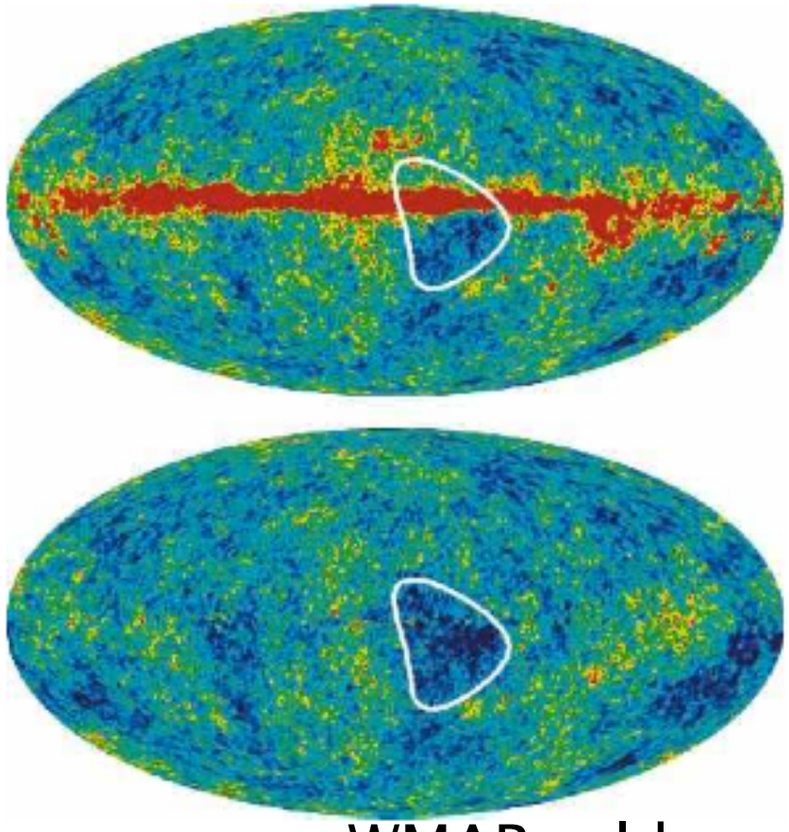

WMAP cold spot

Bennett et al. (2011)

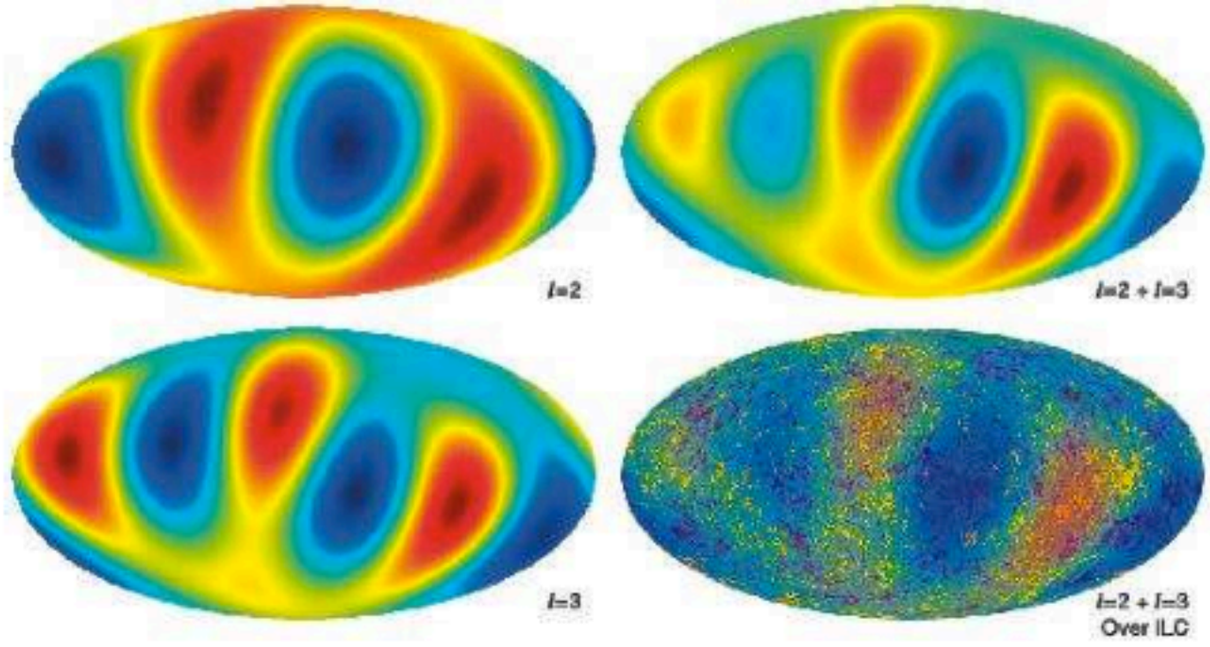

Figure 14. $l = 2$ quadrupole and $l = 3$ octupole maps are added. The combined map is then shown superposed on the ILC map from Figure 2. Note that the quadrupole and octupole components arrange themselves to match the cool fingers and the warm regions in between. The fingers and the alignment of the $l = 2$ and $l = 3$ multipoles are intimately connected.

CMB “anomalies”

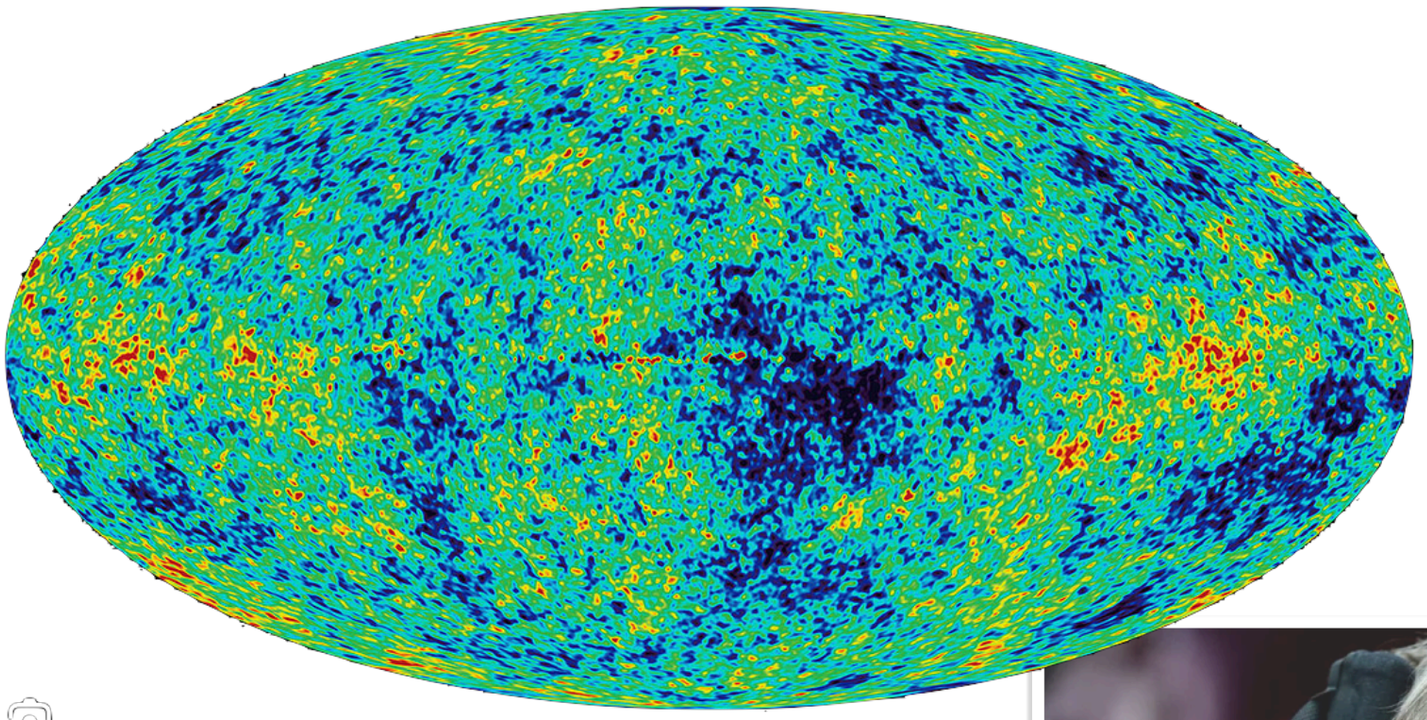

Can you find the initials of Stephen Hawking in this map? 😉

CMB “anomalies”

WMAP 7 yr result
Bennett et al. (2011)

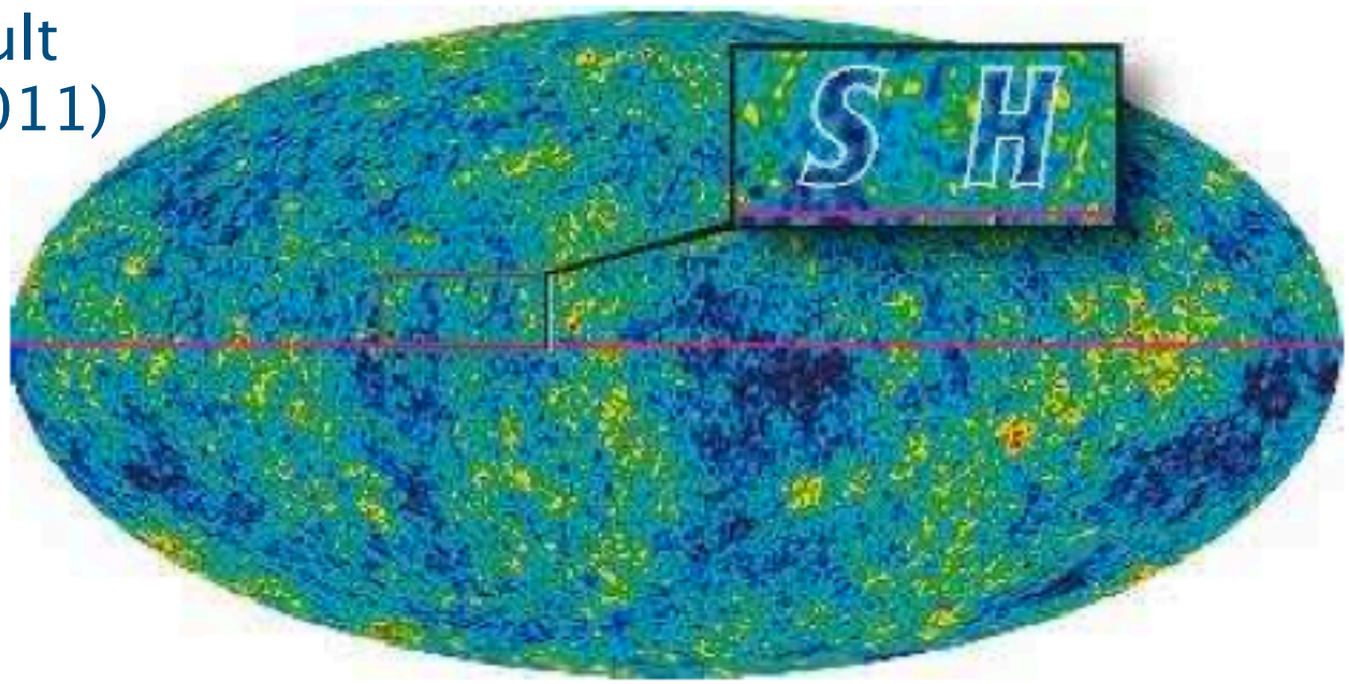

Figure 17. “SH” initials of Stephen Hawking are shown in the ILC sky map. The “S” and “H” are in roughly the same font size and style, and both letters are aligned neatly along a line of fixed Galactic latitude. A calculation would show that the probability of this particular occurrence is vanishingly small. Yet, there is no case to made for a non-standard cosmology despite this extraordinarily low probability event. It is clear that the combined selection of looking for initials, these particular initials, and their alignment and location are all *a posteriori* choices. For a rich data set, as is the case with *WMAP* , there are a lot of data and a lot of ways of analyzing the data. Low probability events are guaranteed to occur. The *a posteriori* assignment of a likelihood for a particular event detected, especially when the detection of that event is “optimized” for maximum effect by analysis choices, does not result in a fair unbiased assessment. This is a recurrent issue with CMB data analysis and is often a tricky issue and one that is difficult to overcome.

CMB “anomalies”

WMAP 7 yr result
Bennett et al. (2011)

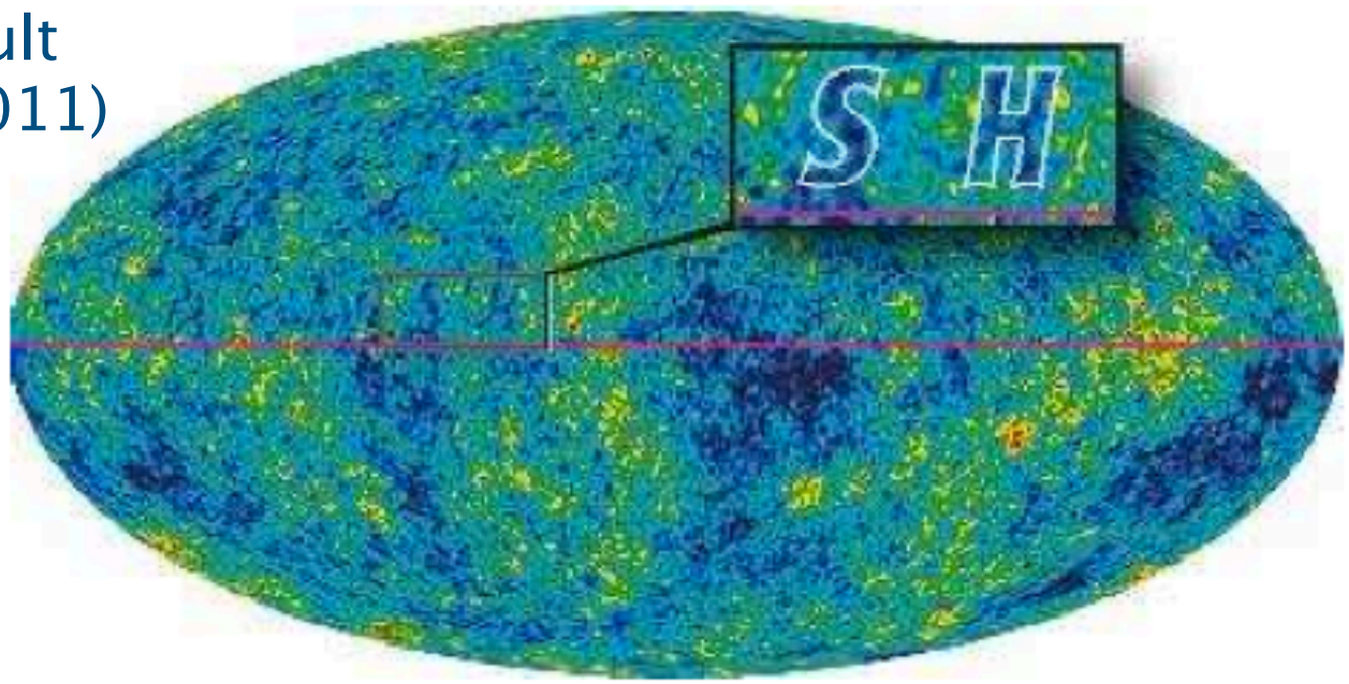

Figure 17. “SH” initials of Stephen Hawking are shown in the ILC sky map. The “S” and “H” are in roughly the same font size and style, and both letters are aligned neatly along a line of fixed

A large fraction of simulated CMB skies will have some kind of anomaly or oddity. The key is whether the oddity is specified in advance.

timized” for maximum effect by analysis choices, does not result in a fair unbiased assessment. This is a recurrent issue with CMB data analysis and is often a tricky issue and one that is difficult to overcome.

“pi” in the sky

Ali Frolop & Douglas Scott, arXiv:1603.09703

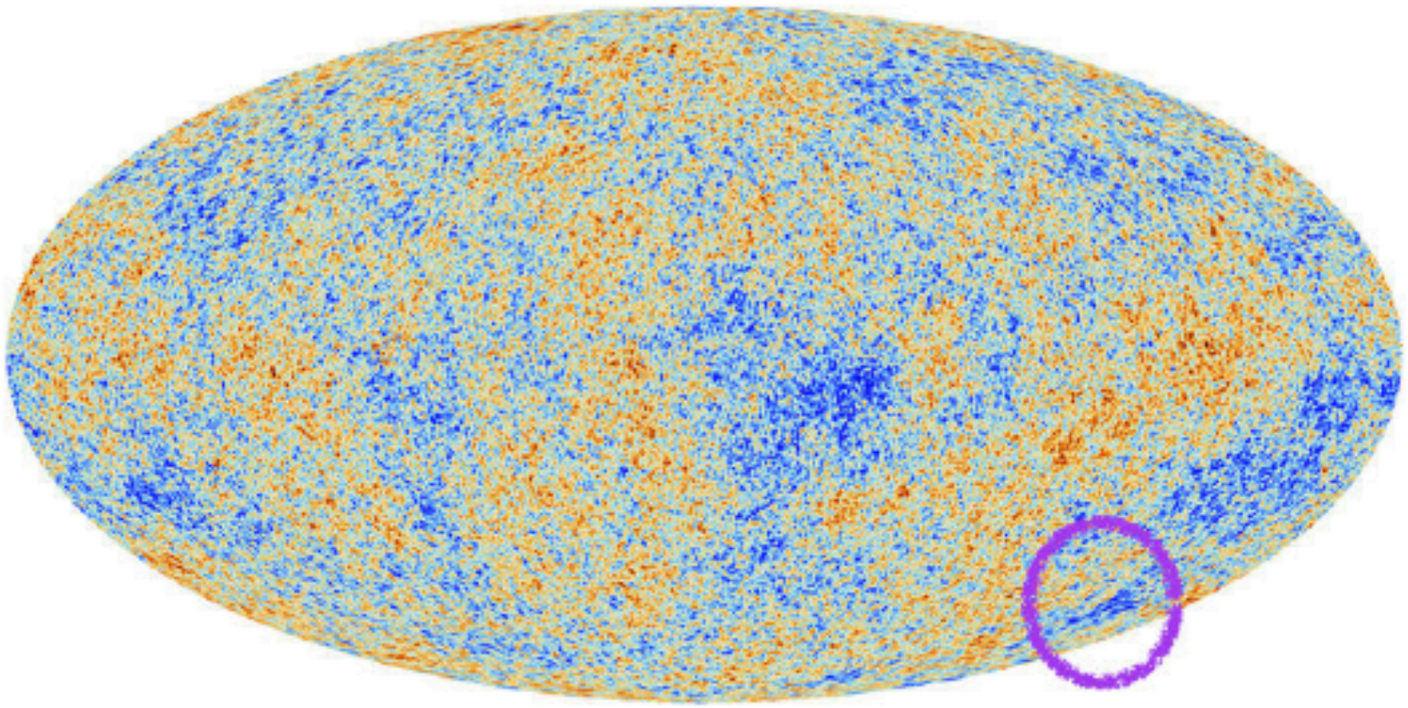

(a)

```
31415926535897932384626433832795028841971693993751 0
58209749445923078164062862089986280348253421170679
82148086513282306647093844609550582231725359408128
48111745028410270193852110555964462294895493038196
44288109756659334461284756482337867831652712019091
45648566923460348610454326648213393607260249141273
72458700660631558817488152092096282925409171536436
78925903600113305305488204665213841469519415116094
33057270365759591953092186117381932611793105118548
07446237996274956735188575272489122793818301194912
98336733624406566430860213949463952247371907021798
60943702770539217176293176752384674818467669405132
00056812714526356082778577134275778960917363717872
14684409012249534301465495853710507922796892589235
42019956112129021960864034418159813629774771309960
51870721134999998372978049951059731732816096318 59
50244594553469083026425223082533446850352619311881
71010003137838752886587533208381420617177669147303
```

(b)

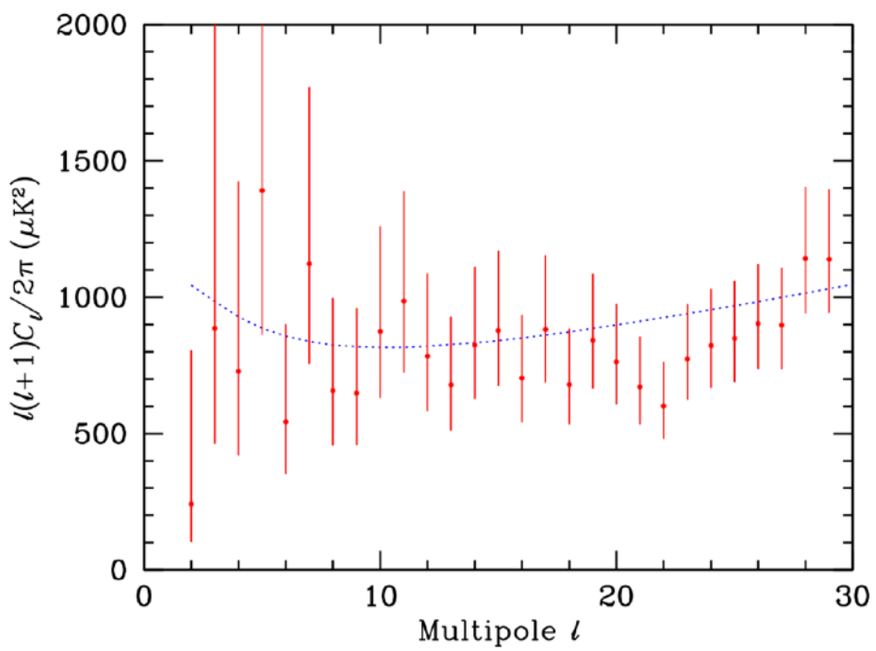

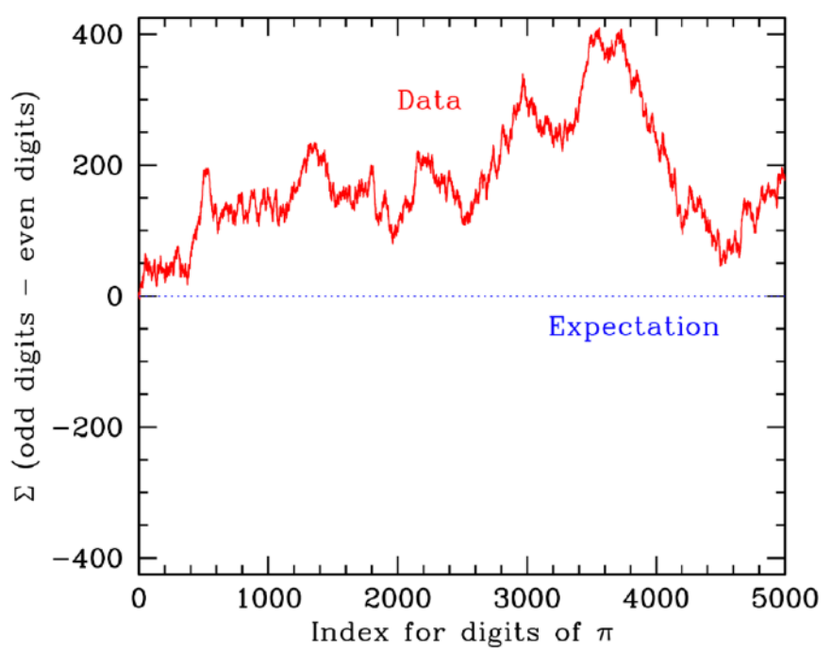

Search for anomalies: Penrose's CCC "rings" in the CMB sky

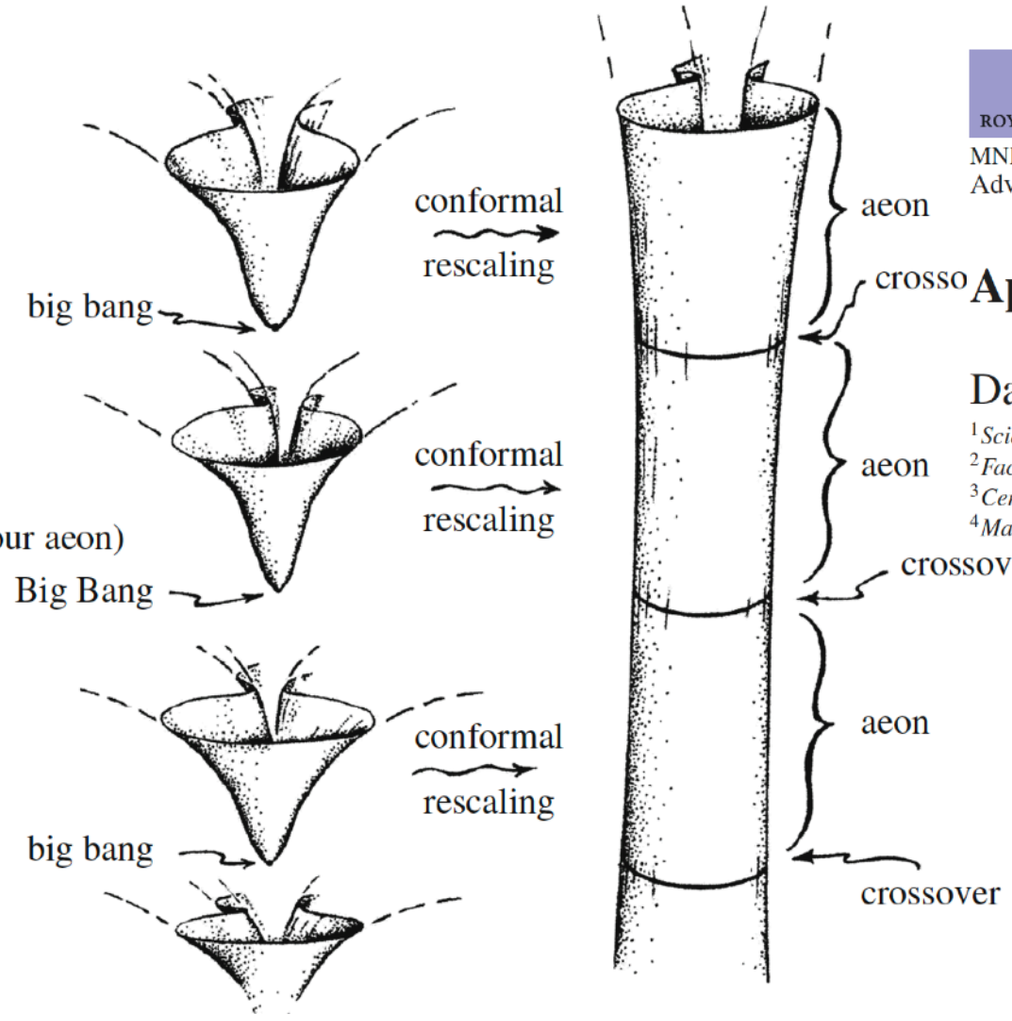

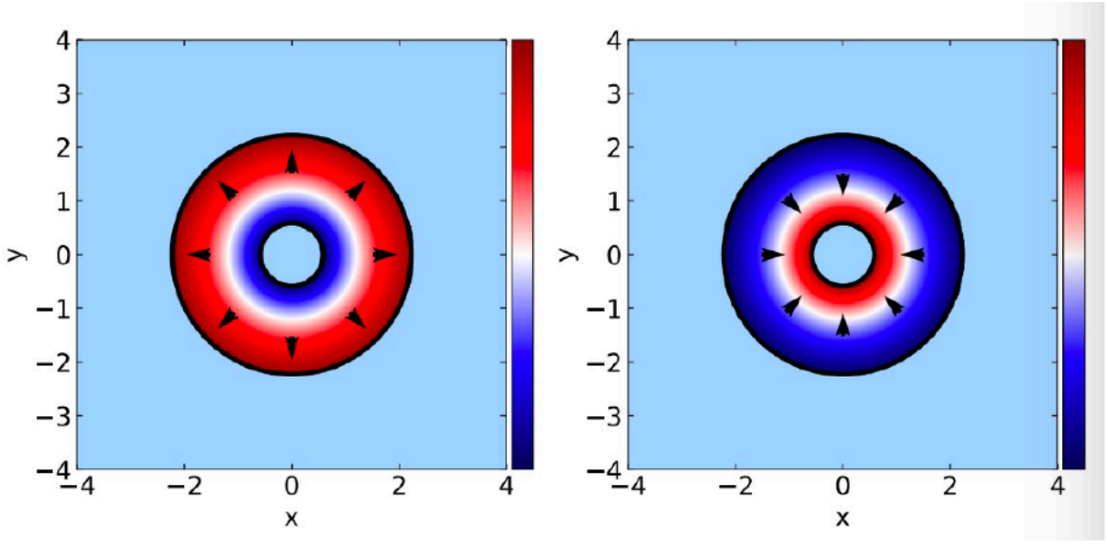

Monthly Notices of the ROYAL ASTRONOMICAL SOCIETY

MNRAS **495,** 3403–3408 (2020) doi:10.1093/mnras/staa1343
Advance Access publication 2020 May 18

Apparent evidence for Hawking points in the CMB Sky★

Daniel An,[1] Krzysztof A. Meissner,[2] Paweł Nurowski[3]† and Roger Penrose[4]

[1] *Science Department, SUNY Maritime College, 6 Pennyfield Av., Throggs Neck, NY 10465, USA*
[2] *Faculty of Physics, University of Warsaw, Pasteura 5, PL-02-093 Warsaw, Poland*
[3] *Center for Theoretical Physics of PAS, Al. Lotników 32/46, PL-02-688 Warsaw, Poland*
[4] *Mathematical Institute, Oxford University, Radcliffe Observatory Quarter, Woodstock Rd., Oxford OX2 6GG, UK*

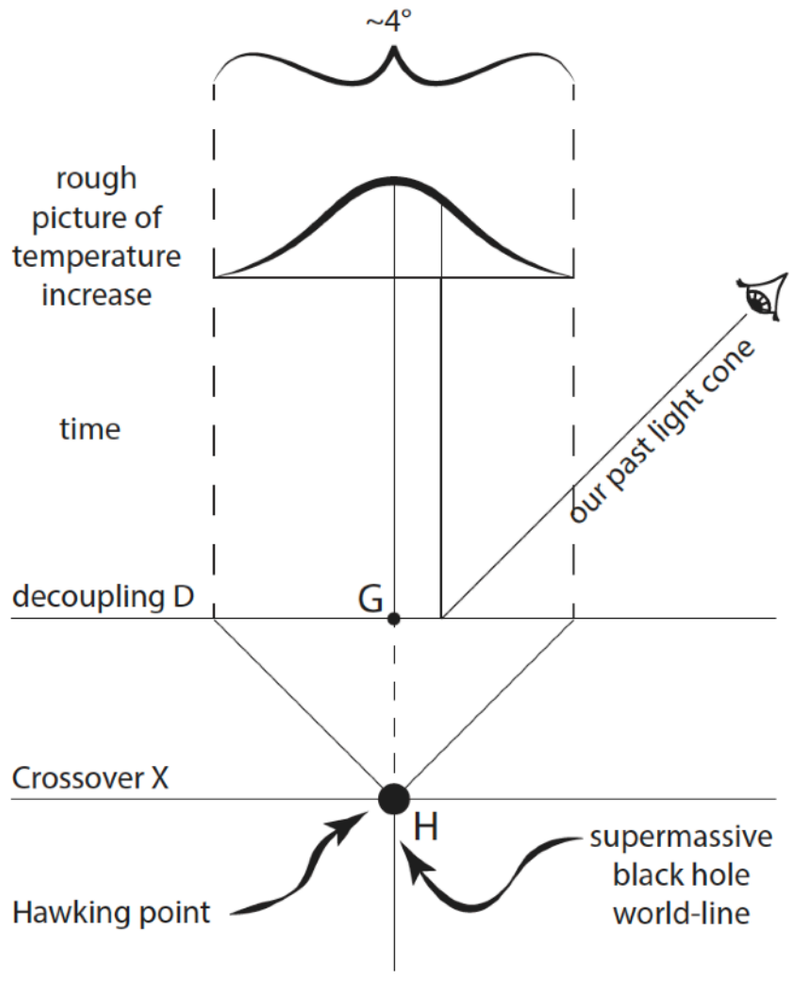

Search for anomalies: Penrose's CCC "rings" in the CMB sky

- Expect a gaussian gradient of the Temperature centred at G
- Look for annular regions in the CMB sky and check for significant drop of temperature from inner to outer boundary of annulus.
- Compare with simulations of randomly generated CMB

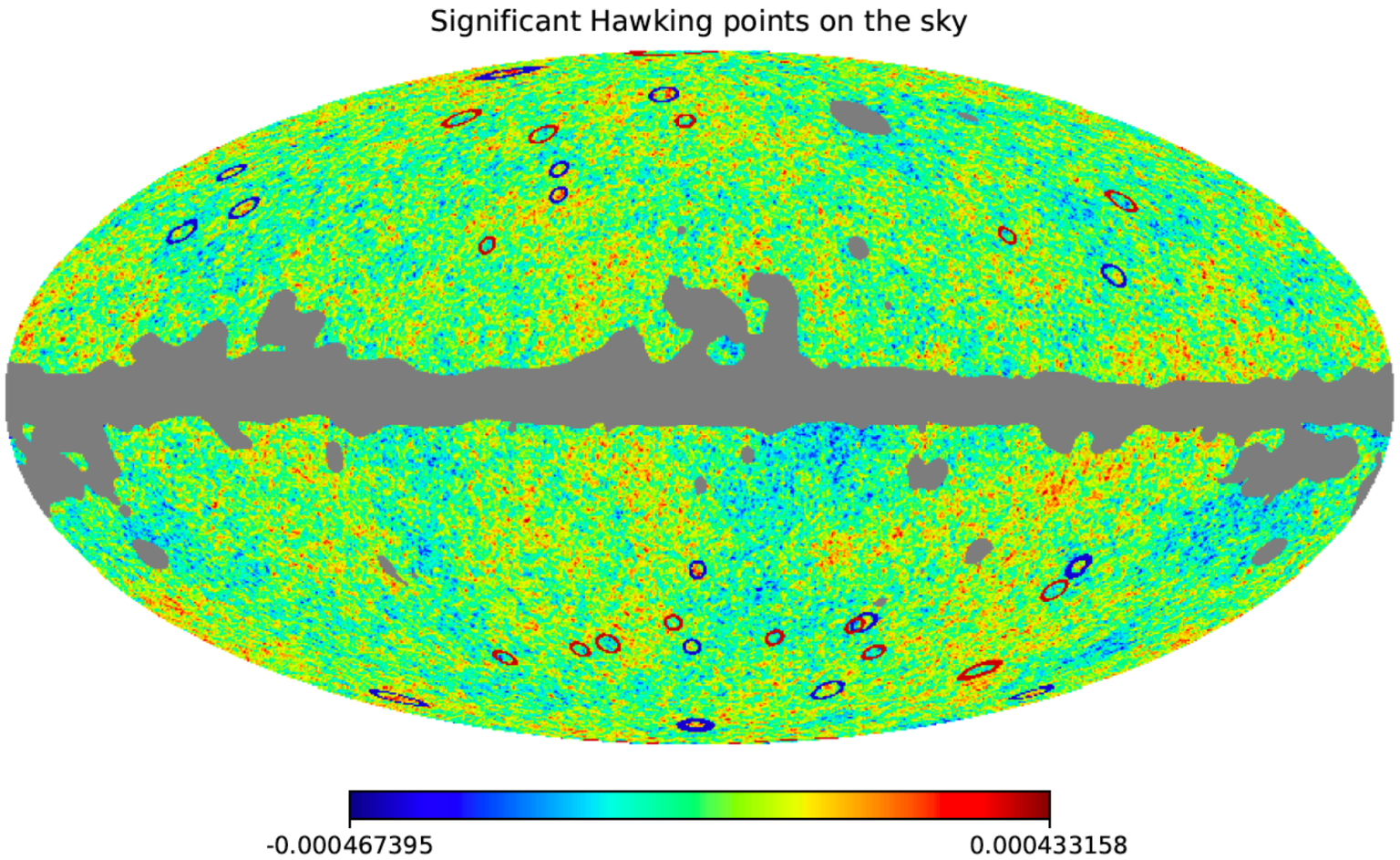

- If marginalized over all possible ring sizes, there is no evidence for "excess" positive-gradient rings (CCC authors do not provide an a-priori size estimate)

- There is no evidence of these rings in the polarization data either

arXiv.org > astro-ph > arXiv:1909.09672

Astrophysics > Cosmology and Nongalactic Astrophysics

[Submitted on 20 Sep 2019 (v1), last revised 21 Jan 2020 (this version, v2)]

Re-evaluating evidence for Hawking points in the CMB

Dylan L. Jow, Douglas Scott

Signs of non-Gaussianity

Gaussian + statistical isotropy

$$\langle \Theta(l_1)\Theta(l_2)\rangle = \delta(l_1 + l_2)C_l$$

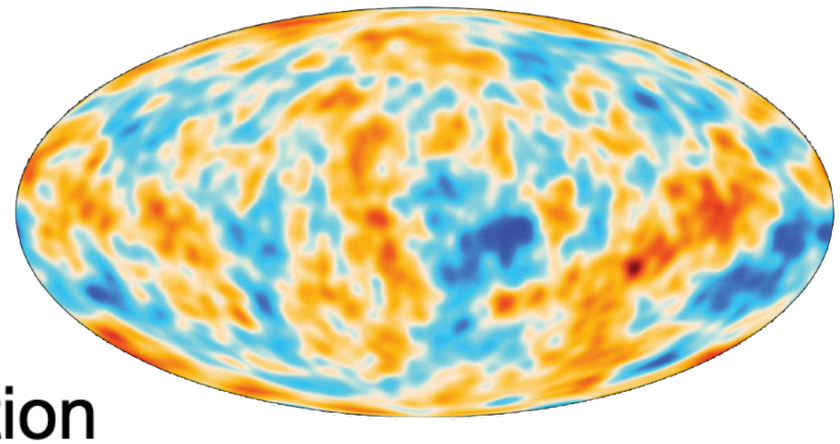

- power spectrum encodes all the information
- modes with different wavenumber are independent

- Primordial non-Gaussianity:
  - Are the initial conditions Gaussian? What is the physics of inflation?
- Intrinsic CMB bispectrum:
  - non-Gaussianity induced by non-linear evolution of perturbations.

Quantifying non-Gaussianity

Bispectrum

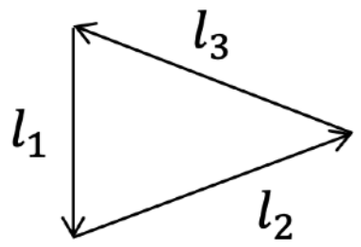

$$\boldsymbol{l_1 + l_2 + l_3 = 0}$$

Flat sky approximation: $\langle \Theta(l_1)\Theta(l_2)\Theta(l_3)\rangle = \frac{1}{2\pi}\delta(l_1 + l_2 + l_3) b_{l_1 l_2 l_3}$

Trispectrum

$$\langle \Theta(\mathrm{l}_1)\Theta(\mathrm{l}_2)\Theta(\mathrm{l}_3)\Theta(\mathrm{l}_4)\rangle_C = (2\pi)^{-2}\delta(\mathrm{l}_1 + \mathrm{l}_2 + \mathrm{l}_3 + \mathrm{l}_4) T(\mathrm{l}_1, \mathrm{l}_2, \mathrm{l}_3, \mathrm{l}_4)$$

$$\langle \Theta(\mathrm{l}_1)\Theta(\mathrm{l}_2)\Theta(\mathrm{l}_3)\Theta(\mathrm{l}_4)\rangle_C = \frac{1}{2}\int \frac{d^2\mathbf{L}}{(2\pi)^2}\delta(\mathrm{l}_1 + \mathrm{l}_2 + \mathbf{L})\delta(\mathrm{l}_3 + \mathrm{l}_4 - \mathbf{L})\mathbb{T}^{(\ell_1\ell_2)}_{(\ell_3\ell_4)}(L) + \text{perms.}$$

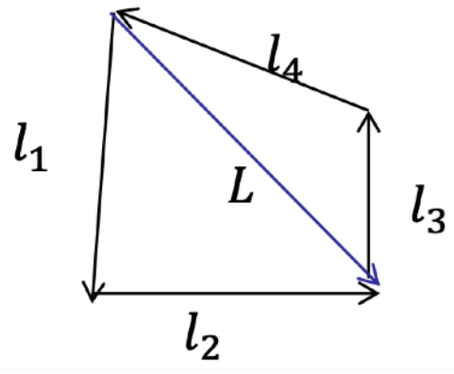

N-spectra…

- Scalar non-Gaussianity

$$\langle \delta(k_1)\delta(k_2)\delta(k_3)\rangle \propto Shape \times f_{NL}$$

Non-Gaussianity from CMB lensing

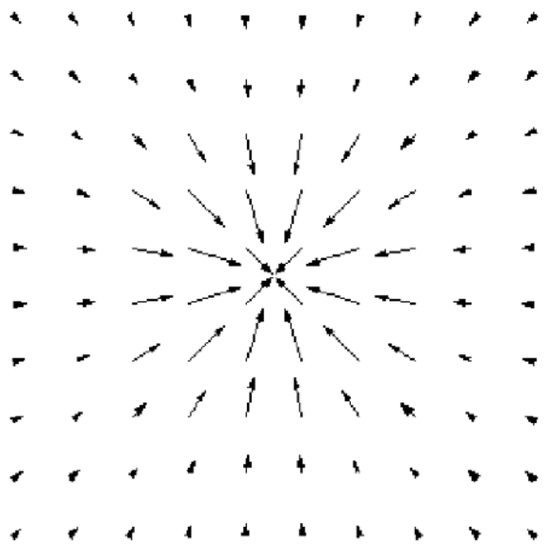

Deflection angles

+

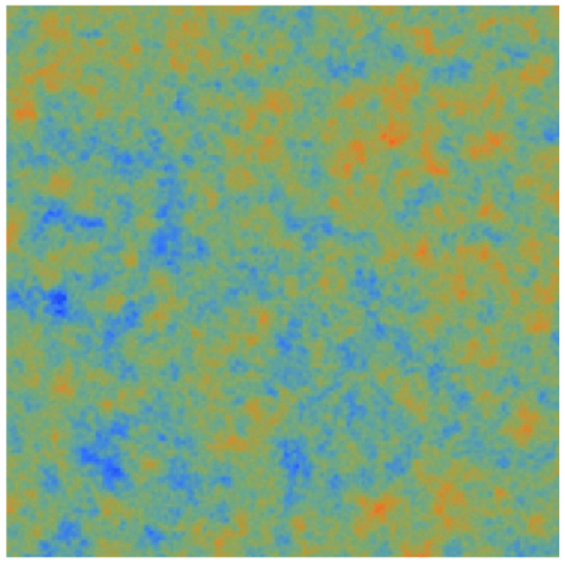

Unlensed CMB

⟶

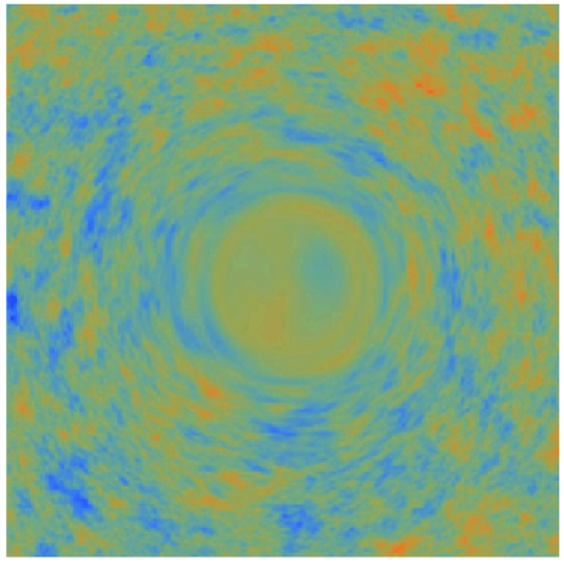

Lensed CMB

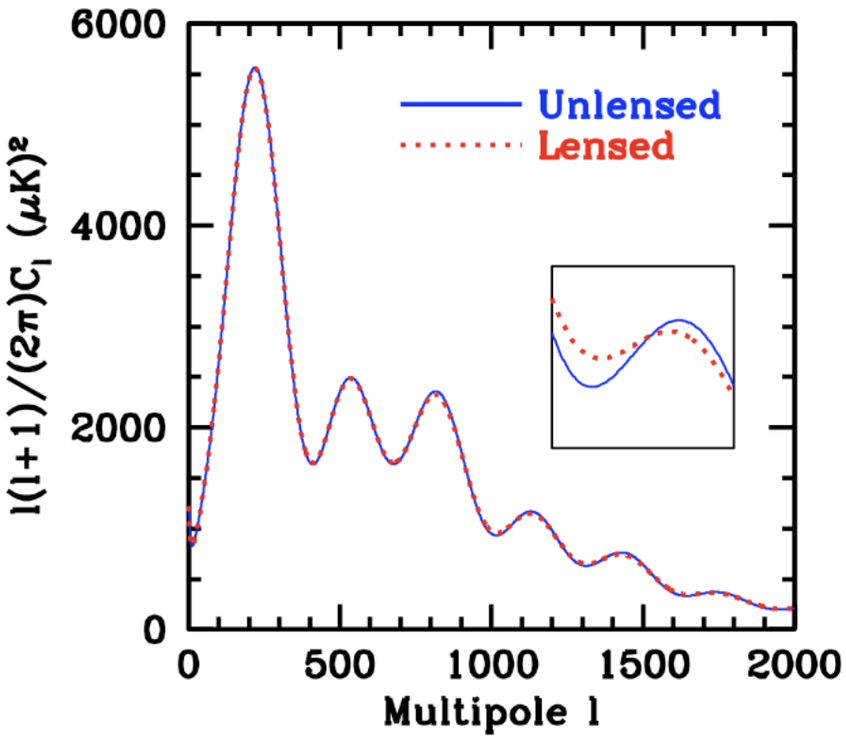

Gravitational lensing correlates the adjacent angular scales and introduces some obvious non-Gaussianity.

But what about other, primordial sources of non-Gaussianity?

- Non-linear velocities during reionization can introduce non-Gaussianities via the kSZ effect
- More interesting is the primordial non-Gaussianities generated during inflation!

Primordial non-Gaussianity

In “vanilla” models of inflation, the initial fluctuations are Gaussian
The 3-point correlation function function is zero:

$$\langle \zeta(k_1)\zeta(k_2)\zeta(k_3)\rangle = 0$$

However, more exotic models can predict nonzero three-point functions
“Local” shape: e.g. curvaton model

$$\zeta(x) = \zeta_G(x) + f_{NL}^{\rm local}\zeta_G(x)^2$$

$$\langle \zeta(k_1)\zeta(k_2)\zeta(k_3)\rangle \sim f_{NL}^{\rm local}\left(\frac{1}{k_1^3 k_2^3} + \text{symm.}\right)\delta^3\left(\sum_i k_i\right)$$

See Bartolo et al. (2012)
arXiv:1001.3957 for a review.

Theoretical models of inflation give us predictions

$$\langle \zeta(k_1)\zeta(k_2)\zeta(k_3)\rangle \propto shape \times f_{NL}$$

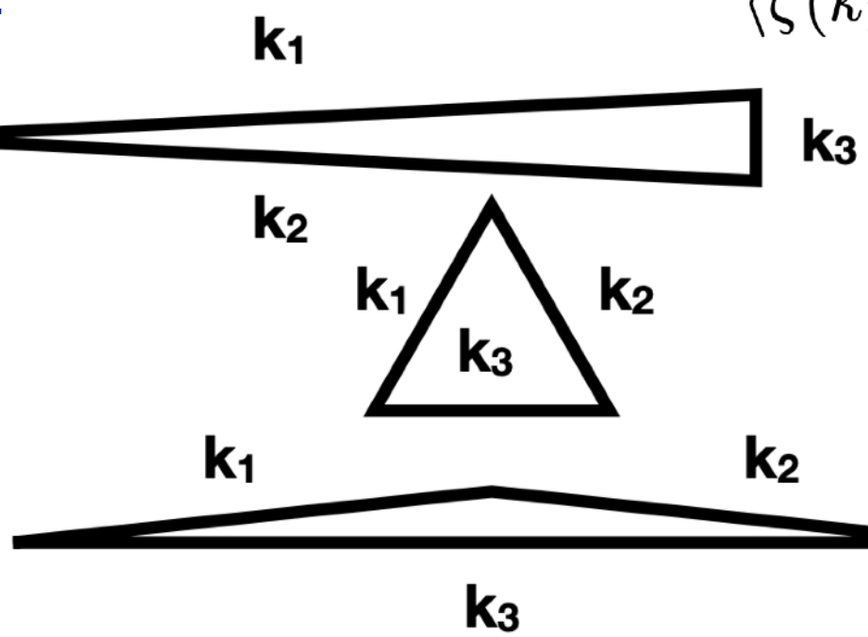

The bispectrum shapes are commonly grouped into three categories: local (squeezed), orthogonal (equilateral), and folded shapes.

f_{NL} to parametrize non-Gaussianity

Primordial non-Gaussianities are generally described by a non-zero value of the three-point correlation function of the primordial curvature function ϕ(k) in the Fourier space:

$$\langle \Phi(\mathbf{k_1})\Phi(\mathbf{k_2})\Phi(\mathbf{k_3})\rangle = (2\pi)^3\delta^{(3)}(\mathbf{k_1}+\mathbf{k_2}+\mathbf{k_3})F(k_1,k_2,k_3)$$

F(k) is the shape function of the bispectrum. In this definition, the primordial curvature perturbations can be parametrized by the dimensionless quantity f_{NL} with respect to the linear Gaussian part in *real space*:

$$\Phi(\mathbf{x}) = \Phi_L(\mathbf{x}) + f_{\mathrm{NL}}\left(\Phi_L^2(\mathbf{x}) - \langle\Phi_L^2(\mathbf{x})\rangle\right)$$

$f_{NL} = 0$

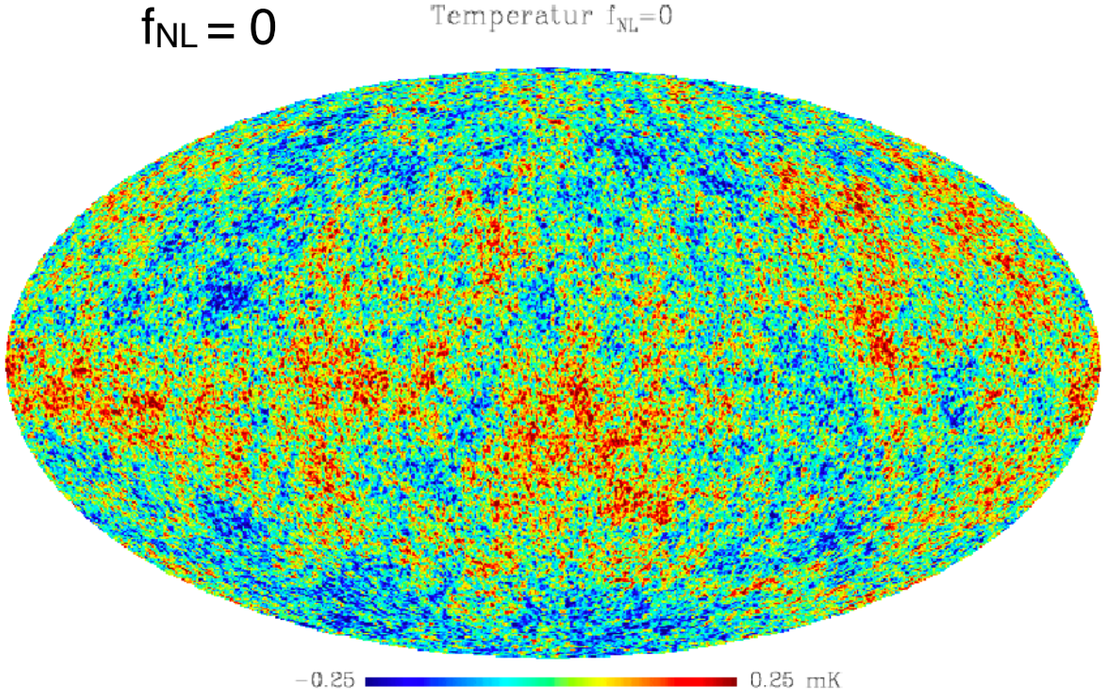

$f_{NL} = 3000$

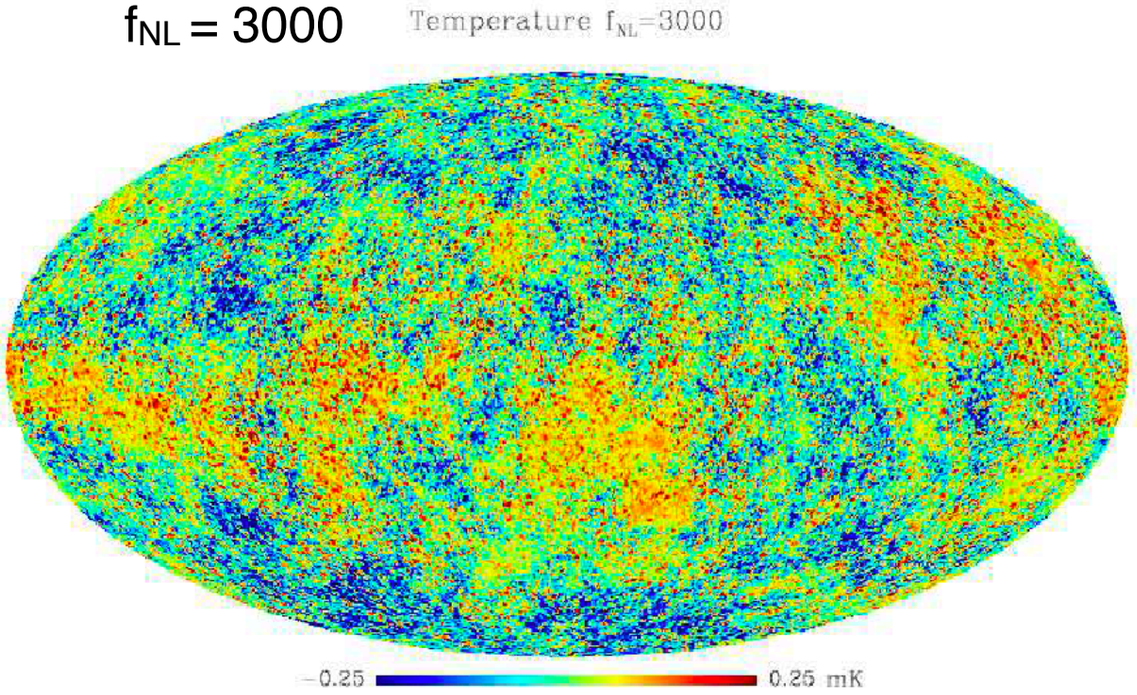

From Liguori et al. (2007)

Planck limits on non-Gaussianity

There is no evidence of a non-zero f_{NL} from Planck data

Planck (2018) results

Temperature bispectrum calculations from different flavors of the CMB maps.

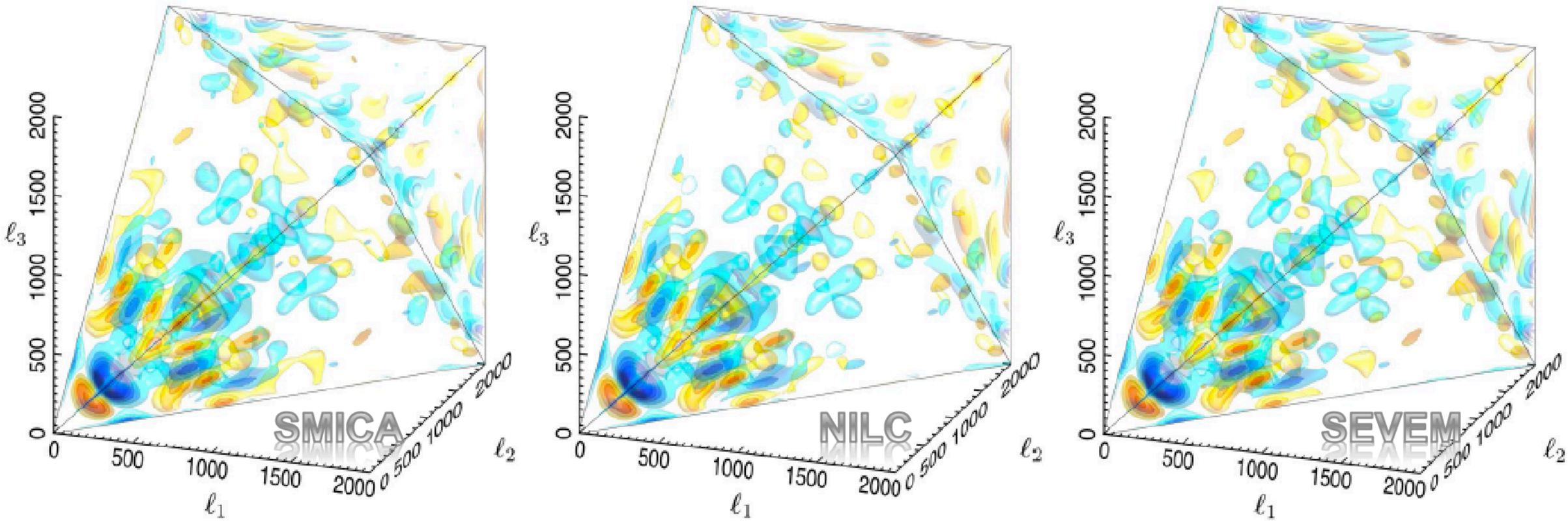

Shape	SMICA		SEVEM		NILC		Commander	
	Independent	Joint	Independent	Joint	Independent	Joint	Independent	Joint
$f_{\rm NL}^{\rm local}$	-0.1 ± 5.6	5.0 ± 8.4	0.0 ± 5.7	1.7 ± 8.7	0.0 ± 5.6	5.2 ± 8.5	-1.3 ± 5.6	3.1 ± 8.3
$f_{\rm NL}^{\rm equil}$	26 ± 69	5 ± 73	43 ± 70	30 ± 74	5 ± 69	-12 ± 73	32 ± 69	20 ± 73
$f_{\rm NL}^{\rm ortho}$	-11 ± 39	-5 ± 44	8 ± 39	13 ± 45	4 ± 39	13 ± 45	29 ± 39	35 ± 44
$b_{\rm PS}/(10^{-29})$	6.3 ± 1.0	5.0 ± 2.7	9.7 ± 1.1	7.1 ± 2.9	5.7 ± 1.1	5.4 ± 2.7	5.4 ± 1.0	3.6 ± 2.6
$A_{\rm CIB}/(10^{-27})$	3.0 ± 0.5	0.6 ± 1.3	4.6 ± 0.5	1.3 ± 1.4	2.6 ± 0.5	0.1 ± 1.3	2.6 ± 0.5	0.9 ± 1.3
$f_{\rm NL}^{\rm dust}/(10^{-2})$	6.6 ± 4.4	6.7 ± 5.9	4.8 ± 4.6	1.9 ± 6.1	4.8 ± 4.4	5.1 ± 5.9	4.4 ± 4.3	3.1 ± 5.7

Questions?

Feel free to email me or ask questions in our eCampus Forum